NASA TM-86282

NASA Technical Memorandum 86282

NASA-TM-86282 19840024806

OPENING OF AN INTERFACE FLAW IN A LAYERED ELASTIC HALF-PLANE UNDER COMPRESSIVE LOADING

JOHN M. KENNEDY, W. B. FICHTER AND JAMES G. GOREE

AUGUST 1984

National Aeronautics and
Space Administration

Langley Research Center
Hampton, Virginia 23665

TABLE OF CONTENTS

LIST OF FIGURES

ABSTRACT

This dissertation presents a static analysis of the problem of an elastic layer perfectly bonded, except for a frictionless interface crack, to a dissimilar elastic half-plane. The free surface of the layer is loaded by a finite pressure distribution directly over the crack. The problem is formulated using the two dimensional linear elasticity equations. Using Fourier transforms, the governing equations are converted to a pair of coupled singular integral equations. The integral equations are reduced to a set of simultaneous algebraic equations by expanding the unknown functions in a series of Jacobi polynomials and then evaluating the singular Cauchy-type integrals. The resulting equations are found to be ill-conditioned and, consequently, are solved in the least-squares sense.

Results from the analysis show that, under a normal pressure distribution on the free surface of the layer and depending on the combination of geometric and material parameters, the ends of the crack can open. The resulting stresses at the crack-tips are singular, implying that crack growth is possible. The extent of the opening and the crack-tip stress intensity factors depend on the width of the pressure distribution zone, the layer thickness, and the relative material properties of the layer and half-plane.

CHAPTER I

INTRODUCTION

Because of their high specific modulus and strength, advanced composite material systems have the potential to reduce the weight of aircraft structures. However, as with any new material system, the mechanical behavior of the material must be understood before it can be used extensively in structures. Understanding the mechanical behavior of composite materials is very challenging because of the complexity of the interactions between fiber and matrix, and between individual plies in a multilayered configuration. With composites have come not only the opportunity for the designer to "tailor" the material to optimize the structure, but also the challenge of a set of potential problems which were largely unknown in metal structures. For example, most of the composite systems are brittle, have low failing strains compared with metals, are susceptible to foreign object impact damage, and can develop delaminations (separation between plies).

Some aspects of the delamination problem are addressed in the present work. Delaminations can be caused by manufacturing deficiencies, standard service loads, or extrinsic loads such as foreign object impacts. The damage which develops from impacts is a complex network of cracked plies, delamination between plies, and broken fibers; and it is very difficult to detect even with ultrasonic or radiographic techniques. A thorough understanding of impact damage is essential, as even small amounts of damage can substantially reduce both the tensile and compressive strength of a composite structure (see, for example, Rhodes [1]).

Considering the delamination problem from the viewpoint of structural life, it must be determined whether the delaminations are likely to grow under subsequent loading and may therefore place limits on either the loads or the life. The problem to be analyzed herein is chosen because it represents a basic mode of failure and should provide an indication of whether a delamination in layered composite materials might grow under the influence of purely compressive loading normal to the delamination. It is felt that a complete solution to the problem using the two-dimensional linear elasticity equations can contribute to a fundamental understanding of the mechanics of delaminations in layered media. Of course, seeking a complete solution necessitates restrictions on the complexity of the geometry and the constitutive equations. In contrast, more complex geometries and loadings can be analyzed using approximate methods such as finite element analysis. However, the power of the stress singularity at the ends of the delamination, a quantity critical to the application of elastic fracture mechanics methods, and other fundamental information on the behavior of the structure would be difficult or impossible to extract from a finite element analysis. The complete solution gives the form of the stress singularity directly from the governing equations. The present solution involves both the concepts of elastic contact problems and the analysis techniques associated with the singular stresses at the ends of the delamination (the delamination is modeled as a crack).

Elasticity solutions of many contact problems and fracture problems involving flaws or cracks have been reported in the literature. For a comprehensive review of contact problems, the reader is referred to Gladwell's recent book [2]. Of particular importance to the present

investigation are papers by Erdogan and his colleagues [3,4,5,6] and Keer et al. [7], in which the frictionless contact between elastic layers and elastic or rigid foundations is studied. All of the above solutions are for either two-dimensional or three-dimensional axisymmetric problems. The layer is of finite thickness and the elastic foundation is either a half-plane or a half-space. The layer is taken to be weightless in all of these studies except in [4] and [5]. The layer rests on the foundation and load is applied to the free surface of the layer either as a compressive normal distributed load or through a stamp. In all of these problems, near the loaded region there is contact between the layer and the foundation. At some distance from the loaded region (on the order of the width of the load or stamp) the layer separates from the foundation and comes back into contact with the foundation only when the weight of the layer is taken into account [5]. The contact stress is typically found to reach a maximum near the center of the loading and to vanish at the ends of the contact zone. The peak contact stress, the width of the contact zone, and the contact stress distribution depend on the layer thickness and the material properties of the layer and foundation. A somewhat different contact problem is solved by Keer and Chantaramungkorn [8]. In this problem, an elastic layer resting on an elastic half-space is loaded by a uniform normal compressive stress over the entire length of the layer except for a finite strip. The important conclusion of the study is that the layer separates from the half-space under the unloaded part of the layer.

In all of these problems there is no bond between the layer and foundation. Thus, the question arises, "How will bonding or partial bonding change the stresses on the interface?" As a prelude to the

present study, the axisymmetric problem solved by Keer et al. [7] was re-examined, using a solution technique similar to that used in [6], to investigate the effect of a modified boundary condition. The physically artificial boundary condition of no separation over a specified radius with zero shear stress was imposed. The three-dimensional axisymmetric solution was then found for a normally loaded elastic layer in contact over a circular region of prescribed radius with an elastic half-space. The results, which are consistent with those in [7], showed that for an arbitrary radius the contact stress was, in general, singular at the edge of the contact zone. However, for certain values of the contact radius the stress was zero at the edge of the contact zone. For contact radii which were about equal to the pressure distribution radius, the contact stresses were compressive, and for greater contact radii, the contact stresses near the end of the contact zone were tensile.

The presence of these regions of tensile stress in the modified problem of [7] and of separation zones [8] under compressive loads suggest that if a layer were subjected to a compressive normal load directly over an interface delamination between the layer and foundation, then the layer could separate from the foundation near the ends of the delamination. Of course, crack opening might be expected only for certain combinations of layer thickness, delamination length, load distribution width, and material properties. It is known that for an opened crack, the crack-tip stresses are tensile and singular and hence the possibility of crack growth, leading to further weakening of the structure, exists. Typically, the magnitude of the stress intensity factors is related to the likelihood of crack growth.

In [9] and [10], the behavior of layered elastic media with flaws, which are idealized as cracks, is studied. A uniform normal compressive stress is applied to both faces of the crack so that the crack is always open. Erdogan [10] finds the well known results that when the materials in the layers are identical the stresses exhibit a square-root singularity, and when the materials are different the stresses exhibit an oscillating square-root singularity. Stress intensity factors are found to depend on layer thickness and material property ratios. One should note that the oscillating singularity, which changes sign an infinite number of times within a small neighborhood of the ends of the crack, is physically unrealistic; yet it is the singularity dictated by the mathematics. The oscillating part of the singularity can be eliminated by modifying the boundary conditions near the ends of the crack [11]. The present problem, however, is formulated with the oscillating singularity, as this does not strongly influence the results away from the crack-tips. The feature of primary interest in the present contact problem is the separation point. Typically, the separation point is outside the region influenced by the oscillatory behavior.

The problem analyzed herein is basically the same problem as that studied in [10] except for the external loading. The geometry is shown in Figure (1a). However, changing the loading complicates the solution considerably. The problem is that of an elastic layer perfectly bonded, except for a crack on the interface, to a dissimilar elastic half-plane. Directly over the crack, uniform normal pressure is applied to the free surface of the layer. The problem is formulated as a two-dimensional elasticity problem; the solution is obtained using the singular integral equation techniques of Erdogan [12]. The integral

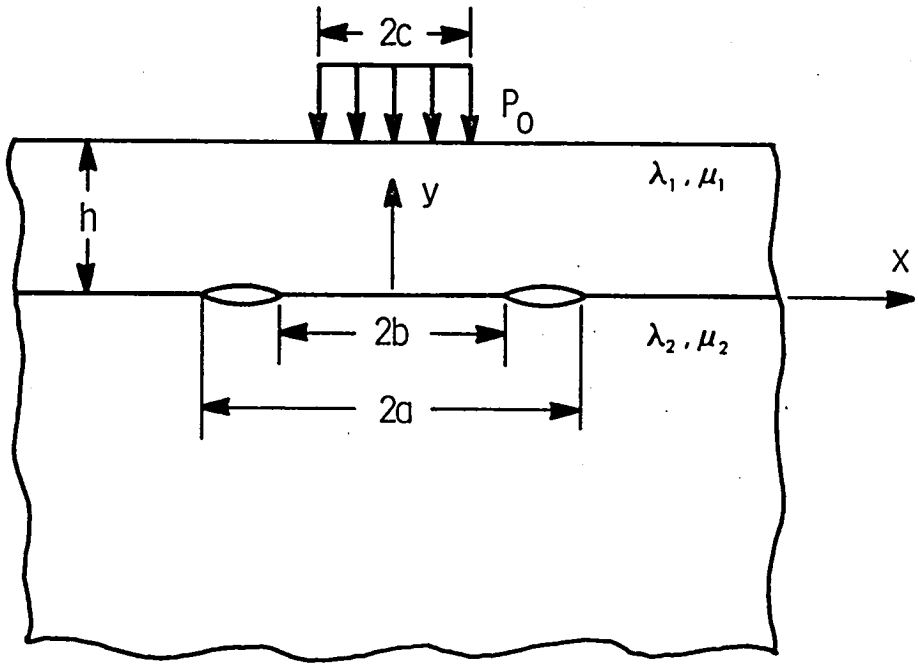

a. Partial-contact.

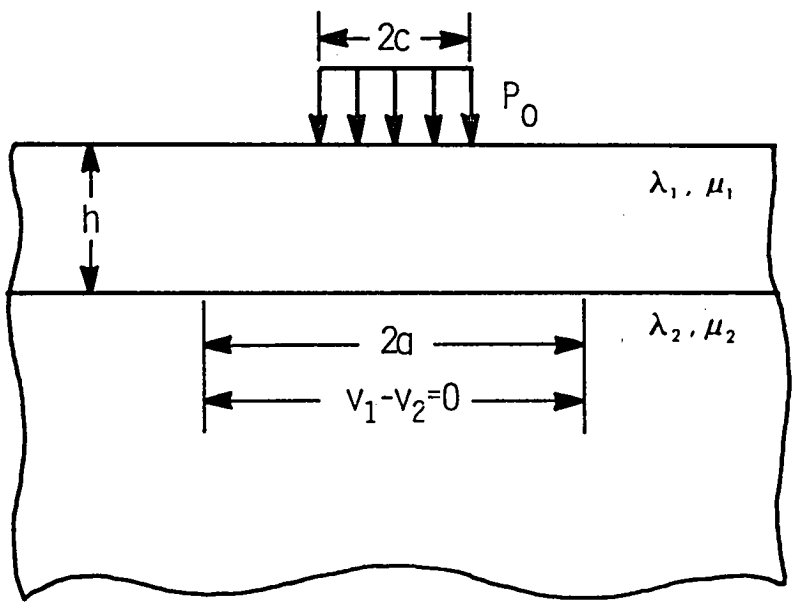

b. Full-contact.

Figure 1. Geometry of the contact problems.

equations derived herein are of the same fundamental form as those in [10]; the difficulty caused by changing the loading shows up in the more complicated boundary conditions in the contact region and in the fact that the extent of the contact region is unknown. The effects of these additional complications on obtaining a solution are discussed later.

The solution gives contact stresses and displacements on the crack faces as well as crack-tip stress intensity factors. The results are presented as functions of material property ratios, the ratio of layer thickness to crack length, and the ratio of pressure distribution width to crack length.

CHAPTER II

FORMULATION

The problem described in the Introduction is formulated using the two-dimensional linear elasticity equations. The solution is obtained by the use of Fourier transforms and singular integral equation techniques as described in [12]. The geometry of the problem is shown in Figure (1a). The layer of thickness h and the half-plane, both isotropic, are assumed to be perfectly bonded along the interface except for a crack of length 2a. The contact between the crack faces is assumed to be frictionless. The load applied to the free surface of the layer is a uniform normal compressive stress, P_o, of width 2c located symmetrically with respect to the crack. The region of primary interest in this problem is the interface. The solution gives stresses and displacements on the interface as well as crack-tip stress intensity factors.

The governing equilibrium equations for the layer (i=1) and the half plane (i=2) are

$$\frac{\partial \sigma_{xx_i}}{\partial x} + \frac{\partial \sigma_{xy_i}}{\partial y} = 0 \quad , \quad \text{and} \tag{1}$$

$$\frac{\partial \sigma_{xy_i}}{\partial x} + \frac{\partial \sigma_{yy_i}}{\partial y} = 0 \tag{2}$$

where σ_{xx_i} and σ_{yy_i} are the normal stresses in the x and y directions, respectively, and σ_{xy_i} is the shear stress. Using the plane strain stress-displacement relations

$$\sigma_{xx_i} = (\lambda_i + 2\mu_i) \frac{\partial u_i}{\partial x} + \lambda_i \frac{\partial v_i}{\partial y} , \tag{3}$$

$$\sigma_{yy_i} = (\lambda_i + 2\mu_i) \frac{\partial v_i}{\partial y} + \lambda_i \frac{\partial u_i}{\partial x} , \quad \text{and} \tag{4}$$

$$\sigma_{xy_i} = \mu_i \left(\frac{\partial v_i}{\partial x} + \frac{\partial u_i}{\partial y} \right), \tag{5}$$

the equilibrium equations become

$$\mu_i \nabla^2 u_i + (\lambda_i + \mu_i) \frac{\partial}{\partial x} \left(\frac{\partial u_i}{\partial x} + \frac{\partial v_i}{\partial y} \right) = 0 , \quad \text{and} \tag{6}$$

$$\mu_i \nabla^2 v_i + (\lambda_i + \mu_i) \frac{\partial}{\partial y} \left(\frac{\partial u_i}{\partial x} + \frac{\partial v_i}{\partial y} \right) = 0 , \tag{7}$$

where λ_i and μ_i are the Lame constants. Multiplying Equation (6) by $\sqrt{2/\pi}\sin(\alpha x)$ and Equation (7) by $\sqrt{2/\pi}\cos(\alpha x)$ and integrating both from zero to infinity yields the transformed equilibrium equations

$$-(\lambda_i + 2\mu_i)\alpha^2 \bar{u}_i + \mu_i \frac{d^2 \bar{u}_i}{dy^2} - (\lambda_i + \mu_i)\alpha \frac{d\bar{v}_i}{dy} = 0 , \quad \text{and} \tag{8}$$

$$(\lambda_i + 2\mu_i) \frac{d^2 \bar{v}_i}{dy^2} - \mu_i \alpha^2 \bar{v}_i + (\lambda_i + \mu_i)\alpha \frac{d\bar{u}_i}{dy} = 0 \tag{9}$$

where $\bar{u}_i$ and $\bar{v}_i$ are the Fourier transforms of u_i and v_i defined by

$$\bar{u}_i(\alpha, y) = \sqrt{\frac{2}{\pi}} \int_0^\infty u_i(x, y) \sin \alpha x \, dx , \quad \text{and} \tag{10}$$

$$\bar{v}_i(\alpha, y) = \sqrt{\frac{2}{\pi}} \int_0^\infty v_i(x, y) \cos \alpha x \, dx . \tag{11}$$

Simultaneous solution of Equations (8) and (9) yields

$$\bar{u}_i = A_i e^{-\alpha y} + B_i y e^{-\alpha y} + C_i e^{\alpha y} + D_i y e^{\alpha y} \quad , \quad \text{and} \tag{12}$$

$$\bar{v}_i = A_i e^{-\alpha y} + B_i \left(\kappa_i \frac{1}{\alpha} + y\right) e^{-\alpha y} - C_i e^{\alpha y} + D_i e^{\alpha y} \left[\kappa_i \frac{1}{\alpha} - y\right] \tag{13}$$

where $\kappa_i = \dfrac{\lambda_i + 3\mu_i}{\lambda_i + \mu_i}$ for plane strain or $\kappa_i = \dfrac{5\lambda_i + 6\mu_i}{3\lambda_i + 2\mu_i}$ for plane stress. The eight arbitrary constants (A_i, B_i, C_i, and D_i) are obtained from the boundary conditions which for the present problem are:

$$\sigma_{xy_1}(x,h) = 0 \quad , \tag{14}$$

$$\sigma_{yy_1}(x,h) = P_o(x) = \begin{cases} -P_o, & |x| \leq c \\ 0, & |x| > c \end{cases} \quad , \tag{15}$$

$$\sigma_{xy_1}(x,0) = \sigma_{xy_2}(x,0) \quad , \tag{16}$$

$$\sigma_{yy_1}(x,0) = \sigma_{yy_2}(x,0) \quad , \tag{17}$$

$$\left.\begin{aligned} u_1(x,0) &= u_2(x,0), \quad |x| > a \\ \sigma_{xy_1}(x,0) &= 0, \quad |x| < a \end{aligned}\right\} , \tag{18}$$

$$\left.\begin{aligned} v_1(x,0) &= v_2(x,0), \quad |x| \leq b \quad \text{and} \quad |x| \geq a \\ \sigma_{yy_1}(x,0) &= 0, \quad b < |x| < a \end{aligned}\right\} , \tag{19}$$

$$u_2(x,-\infty) = 0 \quad , \quad \text{and} \tag{20}$$

$$v_2(x,-\infty) = 0 \quad . \tag{21}$$

The contact distance b in Equation (19) is not known a priori but is found as part of the solution to the integral equations. The mixed boundary conditions, Equations (18) and (19), are difficult to utilize directly in developing a set of simultaneous equations for the eight arbitrary constants. Instead, it is convenient to define two unknown functions

$$f_1(x) = \frac{\partial}{\partial x}\left[u_1(x,0^+) - u_2(x,0^-)\right], \quad \text{and} \tag{22}$$

$$f_2(x) = \frac{\partial}{\partial x}\left[v_1(x,0^+) - v_2(x,0^-)\right] \tag{23}$$

where the + and - superscripts refer to the limiting values of the displacements as y approaches zero from + and - sides, respectively. Using these two definitions in place of the mixed conditions, along with the remaining boundary conditions, Equations (14), (15), (16), (17), (20), and (21), the eight constants in the solutions for $\bar{u}_i$ and $\bar{v}_i$ are obtained. First, from Equations (20) and (21), which require that the displacements vanish for $y \to -\infty$,

$$A_2 = B_2 = 0 .$$

The remaining six constants are obtained from the following six equations written in matrix form:

$$\begin{bmatrix}
-\alpha & -\kappa_1 & \alpha & -\kappa_1 & -\alpha & \kappa_2 \\
\alpha & 0 & \alpha & 0 & -\alpha & 0 \\
\mu_1\alpha & \frac{1}{2}\mu_1(\kappa_1+1) & \mu_1\alpha & -\frac{1}{2}\mu_1(\kappa_1+1) & -\mu_2\alpha & \frac{1}{2}\mu_2(\kappa_2+1) \\
-\mu_1\alpha & -\frac{1}{2}\mu_1(\kappa_1-1) & \mu_1\alpha & -\frac{1}{2}\mu_1(\kappa_1-1) & -\mu_2\alpha & \frac{1}{2}\mu_2(\kappa_2-1) \\
-\alpha e^{-h\alpha} & -\left[h\alpha+\frac{1}{2}(\kappa_1+1)\right]e^{-h\alpha} & -\alpha e^{\alpha h} & \left[-h\alpha+\frac{1}{2}(\kappa_1+1)\right]e^{h\alpha} & 0 & 0 \\
-\alpha e^{-h\alpha} & -\left[h\alpha+\frac{1}{2}(\kappa_1-1)\right]e^{-h\alpha} & \alpha e^{h\alpha} & \left[h\alpha-\frac{1}{2}(\kappa_1-1)\right]e^{h\alpha} & 0 & 0
\end{bmatrix}
\begin{Bmatrix} A_1 \\ B_1 \\ C_1 \\ D_1 \\ C_2 \\ D_2 \end{Bmatrix}
=
\begin{Bmatrix} \bar{f}_2 \\ \bar{f}_1 \\ 0 \\ 0 \\ \frac{\bar{P}_0}{2\mu_1} \\ 0 \end{Bmatrix} \tag{24}$$

where

$$\bar{f}_1(\alpha) = \sqrt{\frac{2}{\pi}} \int_0^\infty f_1(x) \cos(\alpha x) dx \ , \tag{25}$$

$$\bar{f}_2(\alpha) = \sqrt{\frac{2}{\pi}} \int_0^\infty f_2(x) \sin(\alpha x) dx \ , \quad \text{and} \tag{26}$$

$$\bar{P}_o(\alpha) = \sqrt{\frac{2}{\pi}} \int_0^\infty P_0(x) \cos(\alpha x) dx \ . \tag{27}$$

The solution to the six equations was obtained in closed form using MACSYMA, an algebraic manipulative computer code [13]. One should note that the mixed boundary conditions were not satisfied in obtaining the arbitrary constants. Instead, the constants are functions of $\bar{f}_1$ and $\bar{f}_2$, and the mixed boundary conditions are satisfied in formulating the governing integral equations.

The solution to the problem is obtained by developing expressions for the stresses on the interface and then enforcing the mixed boundary conditions on those expressions. This yields two integral equations valid over (-a,a), with unknowns f_1, f_2, the contact stress ($\sigma_{yy}(x,0)$, $|x| < b$), and b. To obtain the integral equations for the interface stresses, only the solutions for C_2 and D_2 are required. They take the form

$$\begin{aligned} C_2 = \frac{1}{\alpha D(\alpha)} \{ & [(c_{11}h\alpha + c_{12})e^{-2h\alpha} + (c_{13}h\alpha + c_{14})e^{-4h\alpha}]\bar{P}_o e^{h\alpha} \\ & + [c_{21} + (c_{22}h^2\alpha^2 + c_{23}h\alpha + c_{24})e^{-2h\alpha} + c_{25}e^{-4h\alpha}]\bar{f}_2 \\ & + [c_{31} + (c_{32}h^2\alpha^2 + c_{33}h\alpha + c_{34})e^{-2h\alpha} + c_{35}e^{-4h\alpha}]\bar{f}_1 \}, \quad \text{and} \end{aligned} \tag{28}$$

$$D_2 = \frac{1}{D(\alpha)} \{[(d_{11}h\alpha + d_{12})e^{-2h\alpha} + (d_{13}h\alpha + d_{14})e^{-4h\alpha}]\bar{P}_o e^{h\alpha}$$

$$+ [d_{21} + (d_{22}h^2\alpha^2 + d_{23}h\alpha + d_{24})e^{-2h\alpha} + d_{25}e^{-4h\alpha}]\bar{f}_2$$

$$+ [d_{31} + (d_{32}h^2\alpha^2 + d_{33}h\alpha + d_{34})e^{-2h\alpha} + d_{35}e^{-4h\alpha}]\bar{f}_1\} \qquad (29)$$

where

$$D(\alpha) = a_{11} + (a_{12}h^2\alpha^2 + a_{13}h\alpha + a_{14})e^{-2h\alpha} + a_{15}e^{-4h\alpha} \; . \qquad (30)$$

and the c_{ij}'s, d_{ij}'s, and a_{ij}'s are defined in Appendix A. In terms of $\bar{u}_i$ and $\bar{v}_i$ the transformed stresses are

$$\bar{\sigma}_{yy_i} = \sqrt{\frac{2}{\pi}} \int_0^\infty \sigma_{yy_i} \cos(\alpha x)dx = (\lambda_i + 2\mu_i) \frac{d\bar{v}_i}{dy} + \lambda_i \alpha \bar{u}_i \; , \qquad (31)$$

$$\bar{\sigma}_{xy_i} = \sqrt{\frac{2}{\pi}} \int_0^\infty \sigma_{xy_i} \sin(\alpha x)dx = \mu_i\left(\frac{d\bar{u}_i}{dy} - \alpha\bar{v}_i\right). \qquad (32)$$

To obtain the expressions for the stresses on the interface, first evaluate $\bar{\sigma}_{yy_2}$ and $\bar{\sigma}_{xy_2}$ as $y \to 0^-$. Then, substituting $\bar{u}_2$ and $\bar{v}_2$ from Equations (12) and (13) into Equations (31) and (32), using Equations (28) and (29), and inverting $\bar{\sigma}_{yy_2}$, $\bar{\sigma}_{xy_2}$, $\bar{P}_o$, $\bar{f}_1$, and $\bar{f}_2$ gives

$$\frac{\pi\sigma_{yy_2}\big|_{y=0^-}}{4\mu_2} = \Bigg[\int_0^\infty P_o(t) \int_0^\infty k_{11}(y,\alpha)\, e^{y\alpha} \cos(\alpha x)\cos(\alpha t)\, d\alpha\, dt$$

$$+ \int_0^\infty f_2(t) \int_0^\infty k_{12}(y,\alpha)\, e^{y\alpha} \cos(\alpha x)\sin(\alpha t)\, d\alpha\, dt \qquad (33)$$

$$+ \int_0^\infty f_1(t) \int_0^\infty k_{13}(y,\alpha)\, e^{y\alpha} \cos(\alpha x)\cos(\alpha t)\, d\alpha\, dt \Bigg]_{y=0^-} \; ,$$

and

$$\frac{\pi\sigma_{xy_2}\big|_{y=0^-}}{4\mu_2} = \left[\int_0^\infty P_o(t)\int_0^\infty k_{21}(y,\alpha)\, e^{y\alpha}\sin(\alpha x)\cos(\alpha t)\, d\alpha\, dt + \int_0^\infty f_2(t)\int_0^\infty k_{22}(y,\alpha)\, e^{y\alpha}\sin(\alpha x)\sin(\alpha t)\, d\alpha\, dt + \int_0^\infty f_1(t)\int_0^\infty k_{23}(y,\alpha)\, e^{y\alpha}\sin(\alpha x)\cos(\alpha t)\, d\alpha\, dt\right]_{y=0^-} \quad (34)$$

where

$$k_{11}(y,\alpha) = \frac{e^{h\alpha}}{D(\alpha)}\{(\beta_{11}h\alpha + \beta_{12})e^{-2h\alpha} + (\beta_{13}h\alpha + \beta_{14})e^{-4h\alpha} - y[d_{12}\alpha e^{-2h\alpha} + (d_{13}h\alpha^2 + d_{14}\alpha)e^{-4h\alpha}]\}\,, \quad (35)$$

$$k_{12}(y,\alpha) = \frac{1}{D(\alpha)}\{\beta_{21} + [\beta_{22}h^2\alpha^2 + \beta_{23}h\alpha + \beta_{24}]e^{-2h\alpha} + \beta_{25}e^{-4h\alpha} - y[d_{21}\alpha + (d_{22}h^2\alpha^3 + d_{23}h\alpha^2 + d_{24}\alpha)e^{-2h\alpha} + d_{25}\alpha e^{-4h\alpha}]\}\,, \quad (36)$$

$$k_{13}(y,\alpha) = \frac{1}{D(\alpha)}\{\beta_{31} + (\beta_{32}h^2\alpha^2 + \beta_{33}h\alpha + \beta_{34})e^{-2h\alpha} + \beta_{35}e^{-4h\alpha} - y[d_{31}\alpha + (d_{32}h^2\alpha^3 + d_{33}h\alpha^2 + d_{34}\alpha)e^{-2h\alpha} + d_{35}\alpha e^{-4h\alpha}]\}\,, \quad (37)$$

$$k_{21}(y,\alpha) = \frac{e^{\alpha h}}{D(\alpha)}\{(\beta_{41}h\alpha + \beta_{42})e^{-2h\alpha} + (\beta_{43}h\alpha + \beta_{44})e^{-4h\alpha} + y[d_{12}\alpha e^{-2h\alpha} + (d_{13}h\alpha^2 + d_{14}\alpha)e^{-4h\alpha}]\}\,, \quad (38)$$

$$k_{22}(y,\alpha) = \frac{1}{D(\alpha)} \{\beta_{51} + (\beta_{52}h^2\alpha^2 + \beta_{53}h\alpha + \beta_{54})e^{-2h\alpha} + \beta_{55}e^{-4h\alpha} + y[d_{21}\alpha + (d_{22}h^2\alpha^3 + d_{23}h\alpha^2 + d_{24}\alpha)e^{-2h\alpha} + d_{25}\alpha e^{-4h\alpha}]\} , \tag{39}$$

and

$$k_{23}(y,\alpha) = \frac{1}{D(\alpha)} \{\beta_{61} + (\beta_{62}h^2\alpha^2 + \beta_{63}h\alpha + \beta_{64})e^{-2h\alpha} + \beta_{65}e^{-4h\alpha} + y[d_{31}\alpha + (d_{32}h^2\alpha^3 + d_{33}h\alpha^2 + d_{34}\alpha)e^{-2h\alpha} + d_{35}\alpha e^{-4h\alpha}]\} . \tag{40}$$

The β_{ij}'s, which are functions of material properties only, are defined in Appendix A.

The fundamental form of the integral equations, Equations (33) and (34), depends on the nature of the integrands of the integrals with respect to α. Recognizing that some of the infinite integrals are not uniformly convergent for $y = 0$, the non-uniformly convergent parts of the integrands are separated from the convergent parts by writing

$$k_{12}(y,\alpha) = \frac{\beta_{21}}{a_{11}} - \frac{d_{21}}{a_{11}} y\alpha - k'_{12}(y,\alpha) , \tag{41}$$

$$k_{13}(y,\alpha) = \frac{\beta_{31}}{a_{11}} - \frac{d_{31}}{a_{11}} y\alpha - k'_{13}(y,\alpha) , \tag{42}$$

$$k_{22}(y,\alpha) = \frac{\beta_{51}}{a_{11}} + \frac{d_{21}}{a_{11}} y\alpha - k'_{22}(y,\alpha) , \quad \text{and} \tag{43}$$

$$k_{23}(y,\alpha) = \frac{\beta_{61}}{a_{11}} + \frac{d_{31}}{a_{11}} y\alpha - k'_{23}(y,\alpha) \tag{44}$$

where the non-uniformly convergent parts are the constant and linear terms in α and the uniformly convergent parts are the primed functions given by

$$k'_{12}(y,\alpha) = \frac{1}{D(\alpha)}\left(e^{-2h\alpha}\left[\left(\beta_{21}\frac{a_{12}}{a_{11}} - \beta_{22}\right)h^2\alpha^2 + \left(\beta_{21}\frac{a_{13}}{a_{11}} - \beta_{23}\right)h\alpha + \left(\beta_{21}\frac{a_{14}}{a_{11}} - \beta_{24}\right)\right] + e^{-4h\alpha}\left(\beta_{21}\frac{a_{15}}{a_{11}} - \beta_{25}\right) + y\alpha\left\{e^{-2h\alpha}\left[\left(d_{22} - d_{21}\frac{a_{12}}{a_{11}}\right)h^2\alpha^2 + \left(d_{23} - d_{21}\frac{a_{13}}{a_{11}}\right)h\alpha + \left(d_{24} - d_{21}\frac{a_{14}}{a_{11}}\right)\right] + e^{-4h\alpha}\left(d_{25} - d_{21}\frac{a_{15}}{a_{11}}\right)\right\}\right), \tag{45}$$

$$k'_{13}(y,\alpha) = \frac{1}{D(\alpha)}\left(e^{-2h\alpha}\left[\left(\beta_{31}\frac{a_{12}}{a_{11}} - \beta_{32}\right)h^2\alpha^2 + \left(\beta_{31}\frac{a_{13}}{a_{11}} - \beta_{33}\right)h\alpha + \left(\beta_{31}\frac{a_{14}}{a_{11}} - \beta_{34}\right)\right] + e^{-4h\alpha}\left(\beta_{31}\frac{a_{15}}{a_{11}} - \beta_{35}\right) + y\alpha\left\{e^{-2h\alpha}\left[\left(d_{32} - d_{31}\frac{a_{12}}{a_{11}}\right)h^2\alpha^2 + \left(d_{33} - d_{31}\frac{a_{13}}{a_{11}}\right)h\alpha + \left(d_{34} - d_{31}\frac{a_{14}}{a_{11}}\right)\right] + e^{-4h\alpha}\left(d_{35} - d_{31}\frac{a_{15}}{a_{11}}\right)\right\}\right), \tag{46}$$

$$k'_{22}(y,\alpha) = \frac{1}{D(\alpha)}\left(e^{-2h\alpha}\left[\left(\beta_{51}\frac{a_{12}}{a_{11}} - \beta_{52}\right)h^2\alpha^2 + \left(\beta_{51}\frac{a_{13}}{a_{11}} - \beta_{53}\right)h\alpha\right.\right.$$

$$\left. + \left(\beta_{51}\frac{a_{14}}{a_{11}} - \beta_{54}\right)\right] + e^{-4h\alpha}\left(\beta_{51}\frac{a_{15}}{a_{11}} - \beta_{55}\right)$$

$$+ y\alpha\left\{e^{-2h\alpha}\left[\left(d_{21}\frac{a_{12}}{a_{11}} - d_{22}\right)h^2\alpha^2 + \left(d_{21}\frac{a_{13}}{a_{11}} - d_{23}\right)h\alpha\right.\right.$$

$$\left.\left. + \left(d_{21}\frac{a_{14}}{a_{11}} - d_{24}\right)\right] + e^{-4h\alpha}\left(d_{21}\frac{a_{15}}{a_{11}} - d_{25}\right)\right\}\Bigg) \quad , \text{ and} \qquad (47)$$

$$k'_{23}(y,\alpha) = \frac{1}{D(\alpha)}\left(e^{-2h\alpha}\left[\left(\beta_{61}\frac{a_{12}}{a_{11}} - \beta_{62}\right)h^2\alpha^2 + \left(\beta_{61}\frac{a_{13}}{a_{11}} - \beta_{63}\right)h\alpha\right.\right.$$

$$\left. + \left(\beta_{61}\frac{a_{14}}{a_{11}} - \beta_{64}\right)\right] + e^{-4h\alpha}\left(\beta_{61}\frac{a_{15}}{a_{11}} - \beta_{65}\right)$$

$$+ y\alpha\left\{e^{-2h\alpha}\left[\left(d_{31}\frac{a_{12}}{a_{11}} - d_{32}\right)h^2\alpha^2 + \left(d_{31}\frac{a_{13}}{a_{11}} - d_{33}\right)h\alpha\right.\right.$$

$$\left.\left. + \left(d_{31}\frac{a_{14}}{a_{11}} - d_{34}\right)\right] + e^{-4h\alpha}\left(d_{31}\frac{a_{15}}{a_{11}} - d_{35}\right)\right\}\Bigg) \quad . \qquad (48)$$

The kernels k_{11} and k_{21} do not contain terms which are constant or linear in α. The non-uniformly convergent parts of the integrand, which can be evaluated in closed form, will provide the basis for determining the fundamental form of f_1 and f_2. Reference [14] evaluates infinite integrals such as those in Equations (33) and (34) with terms which are constant or linear in α. The results are reproduced in Appendix B. Using those results and Equations (41), (42), (43), and (44), the integral equations, Equations (33) and (34), become

$$\frac{\pi\sigma_{yy_2}\ y=0^-}{4\mu_2} = \left(\int_0^\infty P_o(t) \int_0^\infty k_{11}(y,\alpha)\ e^{y\alpha} \cos(\alpha x)\cos(\alpha t)\ d\alpha\ dt \right.$$

$$+ \int_0^\infty f_2(t) \left\{ \frac{\beta_{21}}{2a_{11}} \left[\frac{x+t}{y^2+(x+t)^2} - \frac{x-t}{y^2+(x-t)^2} \right] \right.$$

$$- \frac{d_{21}}{a_{11}} y^2 \left[\frac{x+t}{[y^2+(x+t)^2]^2} - \frac{x-t}{[y^2+(x-t)^2]^2} \right]$$

$$\left. - \int_0^\infty k'_{12}(y,\alpha)\ e^{y\alpha} \cos(\alpha x)\sin(\alpha t)\ d\alpha \right\} dt$$

$$+ \int_0^\infty f_1(t) \left\{ - \frac{\beta_{31}}{2a_{11}} \left[\frac{y}{y^2+(t-x)^2} + \frac{y}{y^2+(t+x)^2} \right] \right.$$

$$+ \frac{d_{31}}{2a_{11}} y \left[\frac{y^2-(t-x)^2}{[y^2+(t-x)^2]^2} + \frac{y^2-(t+x)^2}{[y^2+(t+x)^2]^2} \right]$$

$$\left. \left. - \int_0^\infty k'_{13}(y,\alpha)\ e^{y\alpha} \cos(\alpha x)\cos(\alpha t)\ d\alpha\ dt \right\} dt \right) \Bigg|_{y=0^-} , \qquad (49)$$

and

$$\frac{\pi\sigma_{xy_2}\ y=0^-}{4\mu_2} = \left(\int_0^\infty P_o(t) \int_0^\infty k_{21}(y,\alpha)\ e^{y\alpha} \sin(\alpha x)\cos(\alpha t)\ d\alpha\ dt \right.$$

$$+ \int_0^\infty f_2(t) \left\{ - \frac{\beta_{51}}{2a_{11}} y \left[\frac{1}{y^2+(t-x)^2} - \frac{1}{y^2+(t+x)^2} \right] \right.$$

$$- \frac{d_{21}}{2a_{11}} y \left[\frac{y^2-(t-x)^2}{[y^2+(t-x)^2]^2} - \frac{y^2-(t+x)^2}{[y^2+(t+x)^2]^2} \right]$$

$$\left. - \int_0^\infty k'_{22}(y,\alpha)\ e^{y\alpha} \sin(\alpha x)\sin(\alpha t)\ d\alpha \right\} dt \Bigg)$$

$$+\int_0^\infty f_1(t)\left\{\frac{\beta_{61}}{2a_{11}}\left[\frac{t+x}{y^2+(t+x)^2}-\frac{t-x}{y^2+(t-x)^2}\right]\right.$$

$$+\frac{d_{31}}{a_{11}}y^2\left[\frac{t+x}{[y^2+(t+x)^2]^2}-\frac{t-x}{[y^2+(t-x)^2]^2}\right]$$

$$\left.-\int_0^\infty k'_{23}(y,\alpha)\,e^{y\alpha}\sin(\alpha x)\cos(\alpha t)d\alpha\right\}dt\Bigg)\Bigg|_{y=0^-}. \qquad (50)$$

The integrands of the infinite integrals with respect to α are of negative exponential order for $y < 0$ and the limits exist. The limits of the remaining terms in Equations (49) and (50) are obtained from results in [14] (see Appendix B). Thus, the integral equations become

$$\frac{\pi\sigma_{yy_2}\big|_{y=0^-}}{4\mu_2}=\int_0^\infty P_o(t)\int_0^\infty \kappa_{11}(\alpha)\cos(\alpha x)\cos(\alpha t)\,d\alpha\,dt$$

$$+\frac{\beta_{21}}{2a_{11}}\int_0^\infty f_2(t)\left[\frac{1}{x+t}-\frac{1}{x-t}\right]dt$$

$$-\int_0^\infty f_2(t)\int_0^\infty \kappa_{12}(\alpha)\cos(\alpha x)\sin(\alpha t)d\alpha\,dt$$

$$+\frac{\pi}{2}\frac{\beta_{31}}{a_{11}}f_1(x)-\int_0^\infty f_1(t)\int_0^\infty \kappa_{13}(\alpha)\cos(\alpha x)\cos(\alpha t)d\alpha\,dt\,, \qquad (51)$$

and

$$\frac{\pi\sigma_{xy_2}\Big|_{y=0^-}}{4\mu_2} = \int_0^\infty P_o(t) \int_0^\infty \kappa_{21}(\alpha)\, \sin(\alpha x)\cos(\alpha t)d\alpha\, dt$$

$$+ \frac{\pi}{2}\frac{\beta_{51}}{a_{11}} f_2(x) - \int_0^\infty f_2(t) \int_0^\infty \kappa_{22}(\alpha)\, \sin(\alpha x)\sin(\alpha t)d\alpha\, dt$$

$$+ \frac{\beta_{61}}{2a_{11}} \int_0^\infty f_1(t)\left[\frac{1}{t+x} - \frac{1}{t-x}\right] dt$$

$$- \int_0^\infty f_1(t) \int_0^\infty \kappa_{23}(\alpha)\, \sin(\alpha x)\cos(\alpha t)d\alpha\, dt \qquad (52)$$

where

$$\kappa_{11}(\alpha) = \frac{e^{h\alpha}}{D(\alpha)}\left[e^{-2h\alpha}(\beta_{11}h\alpha + \beta_{12}) + e^{-4h\alpha}(\beta_{13}h\alpha + \beta_{14})\right], \qquad (53)$$

$$\kappa_{12}(\alpha) = \frac{1}{D(\alpha)}\left\{e^{-2h\alpha}\left[\left(\beta_{21}\frac{a_{12}}{a_{11}} - \beta_{22}\right)h^2\alpha^2 + \left(\beta_{21}\frac{a_{13}}{a_{11}} - \beta_{23}\right)h\alpha\right.\right.$$

$$\left.\left. + \left(\beta_{21}\frac{a_{14}}{a_{11}} - \beta_{24}\right)\right] + e^{-4h\alpha}\left(\beta_{21}\frac{a_{15}}{a_{11}} - \beta_{25}\right)\right\}, \qquad (54)$$

$$\kappa_{13}(\alpha) = \frac{1}{D(\alpha)}\left\{e^{-2h\alpha}\left[\left(\beta_{31}\frac{a_{12}}{a_{11}} - \beta_{32}\right)h^2\alpha^2 + \left(\beta_{31}\frac{a_{13}}{a_{11}} - \beta_{33}\right)h\alpha\right.\right.$$

$$\left.\left. + \left(\beta_{31}\frac{a_{14}}{a_{11}} - \beta_{34}\right)\right] + e^{-4h\alpha}\left(\beta_{31}\frac{a_{15}}{a_{11}} - \beta_{35}\right)\right\}, \qquad (55)$$

$$\kappa_{21}(\alpha) = \frac{e^{\alpha h}}{D(\alpha)}\left[e^{-2h\alpha}(\beta_{41}h\alpha + \beta_{42}) + e^{-4h\alpha}(\beta_{43}h\alpha + \beta_{44})\right], \qquad (56)$$

$$\kappa_{22}(\alpha) = \frac{1}{D(\alpha)}\left\{e^{-2h\alpha}\left[\left(\beta_{51}\frac{a_{12}}{a_{11}} - \beta_{52}\right)h^2\alpha^2 + \left(\beta_{51}\frac{a_{13}}{a_{11}} - \beta_{53}\right)h\alpha + \left(\beta_{51}\frac{a_{14}}{a_{11}} - \beta_{54}\right)\right] + e^{-4h\alpha}\left(\beta_{51}\frac{a_{15}}{a_{11}} - \beta_{55}\right)\right\} , \tag{57}$$

$$\kappa_{23}(\alpha) = \frac{1}{D(\alpha)}\left\{e^{-2h\alpha}\left[\left(\beta_{61}\frac{a_{12}}{a_{11}} - \beta_{62}\right)h^2\alpha^2 + \left(\beta_{61}\frac{a_{13}}{a_{11}} - \beta_{63}\right)h\alpha + \left(\beta_{61}\frac{a_{14}}{a_{11}} - \beta_{64}\right)\right] + e^{-4h\alpha}\left(\beta_{61}\frac{a_{15}}{a_{11}} - \beta_{65}\right)\right\} . \tag{58}$$

Noting from the boundary conditions that $f_1(x)$ and $f_2(x)$ are zero for $x > a$, that $P_o(x)$ is zero for $x > c$ and that $f_1(x) = f_1(-x)$, $f_2(x) = -f_2(-x)$, and $P_o(x) = P_o(-x)$, the integral equations can be written as

$$\frac{\pi\sigma_{xy_2}\big|_{y=0^-}}{2\mu_2} = \int_{-c}^{c} P_o(t)\int_0^\infty \kappa_{11}(\alpha)\cos(\alpha x)\cos(\alpha t)d\alpha\,dt + \frac{\beta_{21}}{a_{11}}\int_{-a}^{a}\frac{f_2(t)}{t-x}dt - \int_{-a}^{a} f_1(t)\int_0^\infty \kappa_{12}(\alpha)\cos(\alpha x)\sin(\alpha t)d\alpha\,dt + \pi\frac{\beta_{31}}{a_{11}}f_1(x) - \int_{-a}^{a} f_2(t)\int_0^\infty \kappa_{13}(\alpha)\cos(\alpha x)\cos(\alpha t)d\alpha\,dt, \quad \text{and} \tag{59}$$

$$\frac{\pi\sigma_{yy_2}\big|_{y=0^-}}{2\mu_2} = \int_{-c}^{c} P_o(t)\int_0^\infty \kappa_{21}(\alpha)\sin(\alpha x)\cos(\alpha t)d\alpha\,dt - \frac{\beta_{61}}{a_{11}}\int_{-a}^{a}\frac{f_1(t)}{t-x}dt - \int_{-a}^{a} f_2(t)\int_0^\infty \kappa_{23}(\alpha)\sin(\alpha x)\cos(\alpha t)d\alpha\,dt + \pi\frac{\beta_{51}}{a_{11}}f_2(x) - \int_{-a}^{a} f_1(t)\int_0^\infty \kappa_{22}(\alpha)\sin(\alpha x)\sin(\alpha t)d\alpha\,dt . \tag{60}$$

The equations for $\sigma_{yy_2}\big|_{y=0^-}$ and $\sigma_{xy_2}\big|_{y=0^-}$ are valid for any x on y=0 and the solution for $f_1(x)$ and $f_2(x)$ is obtained by restricting x to the interval (-a,a), i.e., the unbonded portion of the interface.

In addition to the singular integral equations, the continuity conditions

$$u_1(x,0) = u_2(x,0), \qquad |x| > a \ , \quad \text{and} \tag{61}$$

$$v_1(x,0) = v_2(x,0), \qquad |x| > a \tag{62}$$

from the mixed boundary conditions, Equations (18) and (19), require that, in addition to $f_1(x) = f_2(x) = 0$ for $|x| > a$,

$$\int_{-a}^{a} f_1(x)\, dx = 0 \ , \quad \text{and} \tag{63}$$

$$\int_{-a}^{a} f_2(x)\, dx = 0 \tag{64}$$

to prevent a rigid body displacement between the layer and the half-plane. Similarly, to prevent a relative rigid body displacement between the contact region $|x| < b$ and the bonded region $|x| > a$,

$$\int_{-a}^{-b} f_2(x)\, dx = 0. \tag{65}$$

Finally, the part of the mixed boundary condition, Equation (19), which requires continuity of normal displacement over the interior contact region, i.e.,

$$v_1(x,0) = v_2(x,0), \qquad |x| < b, \tag{66}$$

was not satisfied in formulating the integral equations and must be satisfied as an additional constraint on the solution to the integral equations.

Equations (59) and (60), taken over (-a,a), and Equations (63), (64), (65), and (66) provide a complete set of equations to solve for the unknowns $f_1(x)$, $f_2(x)$, and $\sigma_{yy_2}\big|_{y=0}$. The remaining unknown, b, is obtained by an iterative process which is based on the requirement that the contact stress $\sigma_{yy_2}\big|_{y=0}$ vanish at $x = \pm b$. The iterative process is described in Chapter III.

Several fundamentally different problems can be solved using this set of equations. Two of these problems are described below.

Full Contact in the Region (-a,a):

For this problem, $f_2 = 0$ for all x and b = a, which places no restrictions on the sign of the contact stress. The integral equations reduce to a singular integral equation for f_1 and a simple equation for $\sigma_{yy_2}\big|_{y=0}$. Equations (64) and (65) become trivial. The resulting equations and the solution are presented in Appendix C.

No Contact in the Region (-a,a):

Two examples which involve no contact in the region (-a,a) arise (1) when the loading $P_o(x)$ is prescribed as tensile, and (2) when the only prescribed loading is normal pressure on the crack faces, i.e., $\sigma_{yy_2}\big|_{y=0}$ is negative and $\sigma_{xy_2}\big|_{y=0}$ is zero. For these problems the fundamental form of the integral equations does not change, but Equations (65) and (66) are no longer valid boundary conditions. The second problem ($P_o(x) = 0$, $\sigma_{xy_2}\big|_{y=0} = 0$, and $\sigma_{yy_2}\big|_{y=0}$ is compressive) has been solved by Erdogan and Gupta [10].

CHAPTER III

SOLUTION OF THE GOVERNING EQUATIONS

Mixed boundary value problems such as the present one can usually be reduced to a system of singular integral equations with Cauchy-type kernels (such as Equations (59) and (60)). Erdogan et al. [12] give a detailed discussion of techniques for solving equations with Cauchy-type kernels. The present problem is solved using these techniques.

Equations (59) and (60) are singular integral equations of the second kind as defined in [12]. By combining the equations into one complex integral equation, the singular behavior of f_1 and f_2 can be determined from the dominant part of the integral equation. Then, expanding f_1 and f_2 in a series of complex orthogonal polynomials, the singular terms in the integral equation can be removed and the integral equation can be reduced to a system of linear algebraic equations. The present problem has not only the unknowns f_1 and f_2, which appear in the singular integrals, but also $\sigma_{yy}\big|_{y=0}$ and b. Further, the condition on normal displacement in the contact region, Equation (66), adds an additional constraint on f_1 and f_2. The additional unknowns and the constraint equation add considerable complexity to the solution of the problem. The details are discussed as the solution to the problem is developed.

Defining $r = \frac{t}{a}$, $s = \frac{x}{a}$, and

$$g_1(s) = -f_1(as) = -f_1(x), \qquad g_2(s) = f_2(as) = f_2(x)$$

and requiring $|x| < a$, the integral equations become

$$-\frac{a_{11}}{\pi\beta_{21}}\int_{-c}^{c} P_o(t)\int_0^\infty \kappa_{11}(\alpha)\cos(as\alpha)\cos(t\alpha)d\alpha\,dt = \frac{1}{\pi}\int_{-1}^{1}\frac{g_2(r)}{r-s}\,dr$$

$$-\frac{\beta_{31}}{\beta_{21}}g_1(s) + \frac{a}{\pi}\frac{a_{11}}{\beta_{21}}\int_{-1}^{1} g_1(r)\int_0^\infty \kappa_{13}(\alpha)\cos(as\alpha)\cos(ar\alpha)d\alpha\,dr$$

$$-\frac{a}{\pi}\frac{a_{11}}{\beta_{21}}\int_{-1}^{1} g_2(r)\int_0^\infty \kappa_{12}(\alpha)\cos(as\alpha)\sin(ar\alpha)d\alpha\,dr$$

$$-\frac{a_{11}\sigma_{yy_2}(as)\big|_{y=0}}{2\mu_2\beta_{21}}, \qquad |s| < 1, \text{ and} \tag{67}$$

$$-\frac{a_{11}}{\pi\beta_{61}}\int_{-c}^{c} P_o(t)\int_0^\infty \kappa_{21}(\alpha)\sin(as\alpha)\cos(t\alpha)d\alpha\,dt = \frac{1}{\pi}\int_{-1}^{1}\frac{g_1(r)}{r-s}\,dr$$

$$+\frac{\beta_{51}}{\beta_{61}}g_2(s) + \frac{a}{\pi}\frac{a_{11}}{\beta_{61}}\int_{-1}^{1} g_1(r)\int_0^\infty \kappa_{23}(\alpha)\sin(as\alpha)\cos(ar\alpha)d\alpha\,dr$$

$$-\frac{a}{\pi}\frac{a_{11}}{\beta_{61}}\int_{-1}^{1} g_2(r)\int_0^\infty \kappa_{22}(\alpha)\sin(as\alpha)\sin(ar\alpha)d\alpha\,dr, \quad |s| < 1. \tag{68}$$

With the definition

$$\phi(s) = g_2(s) + i\,g_1(s) \tag{69}$$

the integral equations combine to give

$$-\frac{a_{11}}{\pi}\int_{-c}^{c} L(t,s)P_o(t)\,dt = \frac{1}{\pi i}\int_{-1}^{1}\frac{\phi(r)dr}{r-s} + \delta_1\phi(s)$$

$$+\frac{a_{11}}{\pi}\int_{-1}^{1}\left[K_1(r,s)\phi(r) + K_2(r,s)\,\overline{\phi}(r)\right]dr$$

$$+ i\,\delta_2\sigma(s)\big|_{y=0}, \qquad |s| < 1 \tag{70}$$

where

$$L(t,s) = -\int_0^\infty \left[\kappa_{21}(\alpha)\,\sin(as\alpha)\cos(t\alpha) - i\,\kappa_{11}(\alpha)\,\cos(as\alpha)\cos(t\alpha)\right] d\alpha\,, \tag{71}$$

$$K_1(r,s) = \frac{1}{2}\int_0^\infty \left[-\left(\frac{\kappa_{22}(\alpha)}{\beta_{61}}\sin(as\alpha)\sin(ar\alpha) + \frac{\kappa_{13}(\alpha)}{\beta_{21}}\cos(as\alpha)\cos(ar\alpha)\right)\right.$$
$$\left. + i\left(\frac{\kappa_{12}(\alpha)}{\beta_{21}}\cos(as\alpha)\sin(ar\alpha) - \frac{\kappa_{23}}{\beta_{61}}\sin(as\alpha)\cos(ar\alpha)\right)\right] d\alpha, \tag{72}$$

$$K_2(r,s) = \frac{1}{2}\int_0^\infty \left[\left(\frac{\kappa_{13}(\alpha)}{\beta_{21}}\cos(as\alpha)\cos(ar\alpha) - \frac{\kappa_{22}(\alpha)}{\beta_{61}}\sin(as\alpha)\sin(ar\alpha)\right)\right.$$
$$\left. + i\left(\frac{\kappa_{12}(\alpha)}{\beta_{21}}\cos(as\alpha)\sin(ar\alpha) + \frac{\kappa_{23}(\alpha)}{\beta_{61}}\sin(as\alpha)\cos(ar\alpha)\right)\right] d\alpha\,, \tag{73}$$

$$\delta_1 = \frac{\beta_{31}}{\beta_{21}} = \frac{\beta_{51}}{\beta_{61}}\,,\quad \delta_2 = \frac{a_{11}}{2\mu_2\beta_{21}} \quad \text{and} \tag{74}$$

$$\sigma(s) = \sigma_{yy_2}(as)\Big|_{y=0} = \sigma_{yy_1}(as)\Big|_{y=0}\,. \tag{75}$$

Using Equation (69) the continuity Equations (63), (64), and (65), become

$$\int_{-1}^{1} \phi(r)\,dr = 0\,, \quad \text{and} \tag{76}$$

$$\int_{-1}^{-b/a} \mathrm{Re}(\phi(r))\,dr = 0\,, \tag{77}$$

and the constraint equation, Equation (66), becomes

$$\int_{-b/a}^{s} \mathrm{Re}(\phi(r))\, dr = 0, \qquad -\frac{b}{a} < s < \frac{b}{a} . \tag{78}$$

Because K_1, K_2, and L are sums of bounded functions, they are bounded as well. So, the singular behavior of ϕ is determined from the dominant part of the integral equation, i.e., the first two terms on the right-hand side of Equation (70). From [12], this singular behavior has the form

$$w(s) = (1 - s)^{\alpha}(1 + s)^{\bar{\alpha}} , \left(w^*(s) = (1 - s)^{-\alpha}(1 + s)^{-\bar{\alpha}}\right) \tag{79}$$

where

$$\alpha = -\frac{1}{2} - i\,\omega, \quad \bar{\alpha} = -\frac{1}{2} + i\omega, \quad \text{and} \quad \omega = \frac{1}{2\pi} \ell n\left(\frac{1 - \delta_1}{1 + \delta_1}\right). \tag{80}$$

Noting that w(s) is the weight of the Jacobi polynomials [12], it is natural to express the solution of the integral equation as

$$\phi(s) = w(s) \sum_{n=0}^{\infty} C_n\, P_n^{(\alpha,\bar{\alpha})}(s) . \tag{81}$$

From the continuity condition, Equation (76), and the orthogonality relations [15]

$$\int_{-1}^{1} w(t)\, P_n^{(\alpha,\bar{\alpha})}(t)\, P_m^{(\alpha,\bar{\alpha})}(t)\, dx = \begin{cases} 0, & n \neq m \\ \dfrac{2^{\alpha+\bar{\alpha}+1}}{2n + \alpha + \bar{\alpha} + 1} \\ \times \dfrac{\Gamma(n + \alpha + 1)\, \Gamma(n + \bar{\alpha} + 1)}{n!\, \Gamma(n + \alpha + \bar{\alpha} + 1)}, & n = m , \end{cases} \tag{82}$$

it is found that $C_o = 0$.

Substituting Equation (81) into Equation (70) and using the relation

$$\frac{1}{\pi i}\int_{-1}^{1} w(r)\, P_n^{(\alpha,\bar{\alpha})}(r)\,\frac{dr}{r-s} + \delta_1 w(s)\, P_n^{(\alpha,\bar{\alpha})}(s) = \frac{\sqrt{1-\delta_1^2}}{2i}\, P_{n-1}^{(-\alpha,-\bar{\alpha})}(s) \tag{83}$$

from [12], the integral equation reduces to

$$\begin{aligned} -\frac{a_{11}}{\pi}\int_{-c}^{c} L(t,s)\, P_o(t)\, dt = \sum_{n=1}^{\infty}\Bigg\{ & C_n \frac{\sqrt{1-\delta_1^2}}{2i}\, P_{n-1}^{(-\alpha,-\bar{\alpha})}(s) \\ & + \frac{a_{11}}{\pi}\int_{-1}^{1}\Big[K_1(r,s) C_n\, w(r)\, P_n^{(\alpha,\bar{\alpha})}(r) \\ & + K_2(r,s)\,\bar{C}_n\,\bar{w}(r)\,\overline{P_n^{(\alpha,\bar{\alpha})}(r)}\Big]\, dr\Bigg\} \\ & + i\,\delta_2\,\sigma(s), \quad |s| < 1 \end{aligned} \tag{84}$$

where the singularity of the integral equation has been removed.

Recognizing that for partial contact the normal stress on the crack must vanish at the ends of the contact region ($s = \pm b/a$) the stress is represented as

$$\sigma(s) = \begin{cases} 0\,, & |s| > \dfrac{b}{a} \\[2ex] A_o + \displaystyle\sum_{\ell=1}^{L} A_\ell \cos\left[\frac{\pi a s}{2b}(2\ell - 1)\right], & |s| < \dfrac{b}{a} \end{cases} \tag{85}$$

and the proper value of b/a is obtained by requiring that $A_o = 0$.

The unknown C_n's, A_ℓ's, and b can be obtained numerically by reducing Equations (84), (77), and (78) to a set of linear algebraic equations. (The square set of equations generated initially from the governing equations was found to be ill-conditioned. Hence, to obtain a stable set of equations, the constraint equation was overspecified and the equations were solved in the least-squares sense.)

The integral equation, Equation (84), can be reduced to a set of linear equations by expanding both sides of the equation as a series of Jacobi polynomials and then solving for the constant coefficients using the orthogonality relations, Equation (82). The resulting set of equations is

$$\frac{\sqrt{1-\delta_1^2}}{2i}\,\theta_m^{(-\alpha,-\bar{\alpha})}\,C_{m+1}+\sum_{n=1}^{M}\left[B_{nm}\,C_n+D_{nm}\,\bar{C}_n\right]+i\sum_{\ell=0}^{L}S_{\ell m}=R_m\,,$$

$$m=0,1,2,3,\ldots,M \qquad (86)$$

where

$$\theta_m^{(-\alpha,-\bar{\alpha})}=\frac{2^{-\alpha-\bar{\alpha}+1}}{2m-\alpha-\bar{\alpha}+1}\,\frac{\Gamma(m-\alpha+1)\,\Gamma(m-\bar{\alpha}+1)}{m!\,\Gamma(m-\alpha-\bar{\alpha}+1)}\,, \qquad (87)$$

$$B_{nm}=\frac{a\,a_{11}}{\pi}\int_{-1}^{1}w^*(s)\,P_m^{(-\alpha,-\bar{\alpha})}(s)$$

$$\times\int_{-1}^{1}w(r)\,P_n^{(\alpha,\bar{\alpha})}(r)\,K_1(r,s)\,dr\,ds\,, \qquad (88)$$

$$D_{nm} = \frac{a\, a_{11}}{\pi} \int_{-1}^{1} w^*(s)\, P_m^{(-\alpha,-\bar{\alpha})}(s)$$

$$\times \int_{-1}^{1} \bar{w}(r)\, \overline{P_n^{(\alpha,\bar{\alpha})}}(r)\, K_2(r,s)\, dr\, ds\ , \tag{89}$$

$$S_{\ell m} = \delta_2 \begin{cases} A_o \displaystyle\int_{-b/a}^{b/a} w^*(s)\, P_m^{(-\alpha,-\bar{\alpha})}(s)\, ds, & \ell = 0 \\ A_\ell \displaystyle\int_{-b/a}^{b/a} w^*(s)\, P_m^{(-\alpha,-\bar{\alpha})}(s) \cos\left[\frac{\pi a s}{2b}(2\ell - 1)\right] ds\ , & \ell = 1,2,\ldots,L\ , \text{ and} \end{cases} \tag{90}$$

$$R_m = -\frac{a_{11}}{\pi} \int_{-1}^{1} w^*(s)\, P_m^{(-\alpha,-\bar{\alpha})}(s) \int_{-c}^{c} P_o(t)\, L(t,s)\, dt\, ds\ . \tag{91}$$

The continuity equation, Equation (77) after substitution of Equation (81), can be integrated in closed form using the definition of the Jacobi polynomials [15]. The result is

$$0 = \mathrm{Re} \sum_{n=1}^{M} C_n \frac{(-1)^n}{2n} \left(1 - \frac{b}{a}\right)^{\bar{\alpha}+1} \left(1 + \frac{b}{a}\right)^{\alpha+1} P_{n-1}^{(\bar{\alpha}+1,\alpha+1)}\left(\frac{b}{a}\right)\ . \tag{92}$$

The constraint equation, Equation (78), also can be integrated in closed form and then both sides of the resulting equation can be expanded as series of Chebyshev polynomials [15] with constant coefficients. The coefficients are evaluated using the orthogonality relations for Chebyshev polynomials [15]. The resulting set of equations is

$$0 = \mathrm{Re} \sum_{n=1}^{M} C_n \int_{-b/a}^{b/a} I_n(r) \sqrt{1 - \left(\frac{ar}{b}\right)^2}\, U_q\left(\frac{a}{b} r\right) dr, \quad q = 0,1,2,\ldots,Q \tag{93}$$

where

$$I_n(r) = \frac{1}{2n}\left[(-1)^{n+1}\left(1 - \frac{b}{a}\right)^{\bar{\alpha}+1}\left(1 + \frac{b}{a}\right)^{\alpha+1} P_{n-1}^{(\bar{\alpha}+1,\alpha+1)}\left(\frac{b}{a}\right)\right.$$

$$\left. - (1 - r)^{\alpha+1}\,(1 + r)^{\bar{\alpha}+1}\,P_{n-1}^{(\alpha+1,\bar{\alpha}+1)}(r)\right] \qquad (94)$$

and $U_q\left(\frac{a}{b}\,r\right)$ is the Chebyshev polynomial of the second kind.

The Equations (86), (92), and (93) yield M + Q + 1 linear algebraic equations for determination of M C_n's, and L + 1 A_ℓ's. The C_n's and A_ℓ's are sufficient to determine the stresses and displacements along the entire interface, y = 0. Recognizing that the stresses on the interface are singular at s = ±1, the complex stress intensity factor is defined to be [10]

$$k_1 + i\,k_2 = \lim_{x\to 1^+} (x - 1)^{-\alpha}\,(x + 1)^{-\bar{\alpha}}\left(\sigma_{yy_2}\Big|_{y=0} + i\,\sigma_{xy_2}\Big|_{y=0}\right). \qquad (95)$$

Following [10], the stress intensity factors are computed from

$$k_1 + i\,k_2 = \frac{-\mu_1\mu_2\left[\mu_1(1 + \kappa_2) + \mu_2(1 + \kappa_1)\right]}{(\mu_1 + \mu_2\kappa_1)(\mu_2 + \mu_1\kappa_2)}\sqrt{1 - \delta_1^2}\sum_{n=1}^{M} C_n\,P_n^{(\alpha,\bar{\alpha})}(1)\ . \qquad (96)$$

The set of simultaneous Equations (86), (92), and (93) must be solved numerically to obtain the C_n's and A_n's. As mentioned previously, these equations were found to be ill-conditioned when L = Q [16]. Thus, a solution was sought by making Q > L and satisfying the equations in a least-squares sense [16]. Reasonable answers were then obtained. The condition of the set of equations was found to be further improved by setting M >> L. This is consistent with the nature of the boundary conditions on the crack surface. The series on g_2 has M terms to

represent both the zero displacement difference in the region $(-b/a,b/a)$ and the non-zero displacement difference in the regions $(-1,-b/a)$ and $(b/a,1)$; however, the stress, $\sigma(s)$ which has L terms, can be represented by only a few terms because it is smooth and symmetric.

To obtain a valid solution to the problem, the value of b was incremented until $|A_0| < \varepsilon$ where a satisfactory value of ε depended on h. The solution was assumed to have converged when solutions with different values for M and L gave b's which differed by less than one percent.

The integrals in Equations (88), (89), (90), (91), and (93) were evaluated using quadrature formulas. Integrals with $(1 - x^2)^{\pm 1/2}$ behavior near the end points were integrated using the Gauss-Chebyshev integration formulas [17]. The infinite integrals ($K_1(r,s)$ and $K_2(r,s)$) were integrated using the Gauss-Legendre integration formula [17].

CHAPTER IV

RESULTS AND DISCUSSION

No Contact in the Region (-a,a)

In this problem a crack of length 2a on the interface between the layer and the half-plane is opened by a unit normal pressure applied to both faces. The governing integral equations are given by Equations (59) and (60) with $P_o(x) = 0$ and $\sigma_{yy_2}\big|_{y=0} = -1$. This problem, which was first solved in [10], was re-solved herein to check the formulation and programming of the partial-contact problem.

In [10] stress intensity factors (for various values of h/2a) are presented for an epoxy layer and an aluminum half-plane (see Figure (6) in [10]). Corresponding results from the present formulation were found to be in excellent agreement with those results.

A second check can be obtained by specifying identical elastic properties for the layer and the half-plane. For this problem the infinite integrals in Equations (59) and (60) can be evaluated in closed form. The resulting expressions are identical to those given by Equation (7.93) of [12], except for the sign of $k_{21}(x,t)$. It was verified in correspondence with Professor Erdogan that the minus sign had been omitted in [12].

The solutions of these two problems provide a check on the entire formulation of the partial-contact problem except for the terms involving $P_o(x)$. They also validate the reduction of the integral equations to simultaneous algebraic equations as well as the programming of the solution.

Full Contact in the Region (-a,a)

This problem contains the physically unrealistic boundary condition of frictionless adherence of the layer and the half-plane (see Figure (1b)). The resulting integral equations are considerably simplified, and they are readily solved numerically. Details of the formulation and solution of this problem are in Appendix C. This auxiliary problem was solved to obtain an initial estimate of the separation point in the partial-contact problem. In fact, in all cases the point where the contact stress changed sign in the full-contact problem was an upper bound for the separation point in the partial-contact problem.

Interestingly, the integral equations for the two problems differ considerably. The full-contact problem is governed by a single integral equation of the first kind, while the partial-contact problem is governed by a pair of integral equations of the second kind. In the full-contact problem, the stresses are singular at the crack-tip. The normal stress, $\sigma_{yy}|_{y=0}$, is singular as the crack-tip is approached from within the crack and non-singular as the crack-tip is approached from the bonded side. On the other hand, the shear stress, $\sigma_{xy}|_{y=0}$, which is of course zero along the crack, is singular as the crack-tip is approached from the bonded side. This behavior of the stresses near a closed crack-tip has been discussed by Comninou [11]. In the partial-contact problem, the stresses have an oscillating square root singularity at the crack-tip. Both $\sigma_{yy}(x,o)$ and $\sigma_{xy}(x,o)$ are singular as the crack-tip is approached from the bonded side and, as the boundary conditions require, they are zero on the crack faces near the crack-tip.

The contact stresses on the crack are shown in Figure (2) for the case of a steel layer and an aluminum half-plane and in Figure (3) for the case of an aluminum layer and a steel half-plane. Both figures show normalized contact stresses versus position on the crack for several values of $\frac{h}{a}$. As is typical for contact between layers, the magnitude of the stress is largest for thin layers and it is concentrated under the applied pressure. For thicker layers the stress is distributed over a larger area. For the case of a steel layer and an aluminum half-plane (Figure (2)), the contact stress for the given geometries is compressive over the entire crack and at the crack-tip the stress is singular in compression. This behavior is typical for cases where $E_1 > E_2$ and $\frac{c}{a} > 0.3$. When $\frac{c}{a}$ and $\frac{h}{a}$ are small the stress distribution can have a region of tensile stress near the ends of the crack. However, the singular contact stress at the crack-tips is always compressive. For the case of an aluminum layer and a steel half-plane (Figure (3)), the contact stress is compressive over most of the crack and tensile near the crack-tip; the stress at the crack-tip is singular in tension. The point where the contact stress changes sign moves toward the crack-tip as the layer thickness increases.

Figures (2) and (3) show that, if the modulus of the layer is greater than that of the half-plane, the singular stress is compressive, but that if this relationship is reversed, the singular stress is tensile. If the material properties are identical, the contact stress at the crack-tip is non-singular. This can be seen by examining the free term in Equation (C.1), which determines the contact-stress singularity. The material property coefficient, β_{31}, of the free term is zero when the material properties are identical.

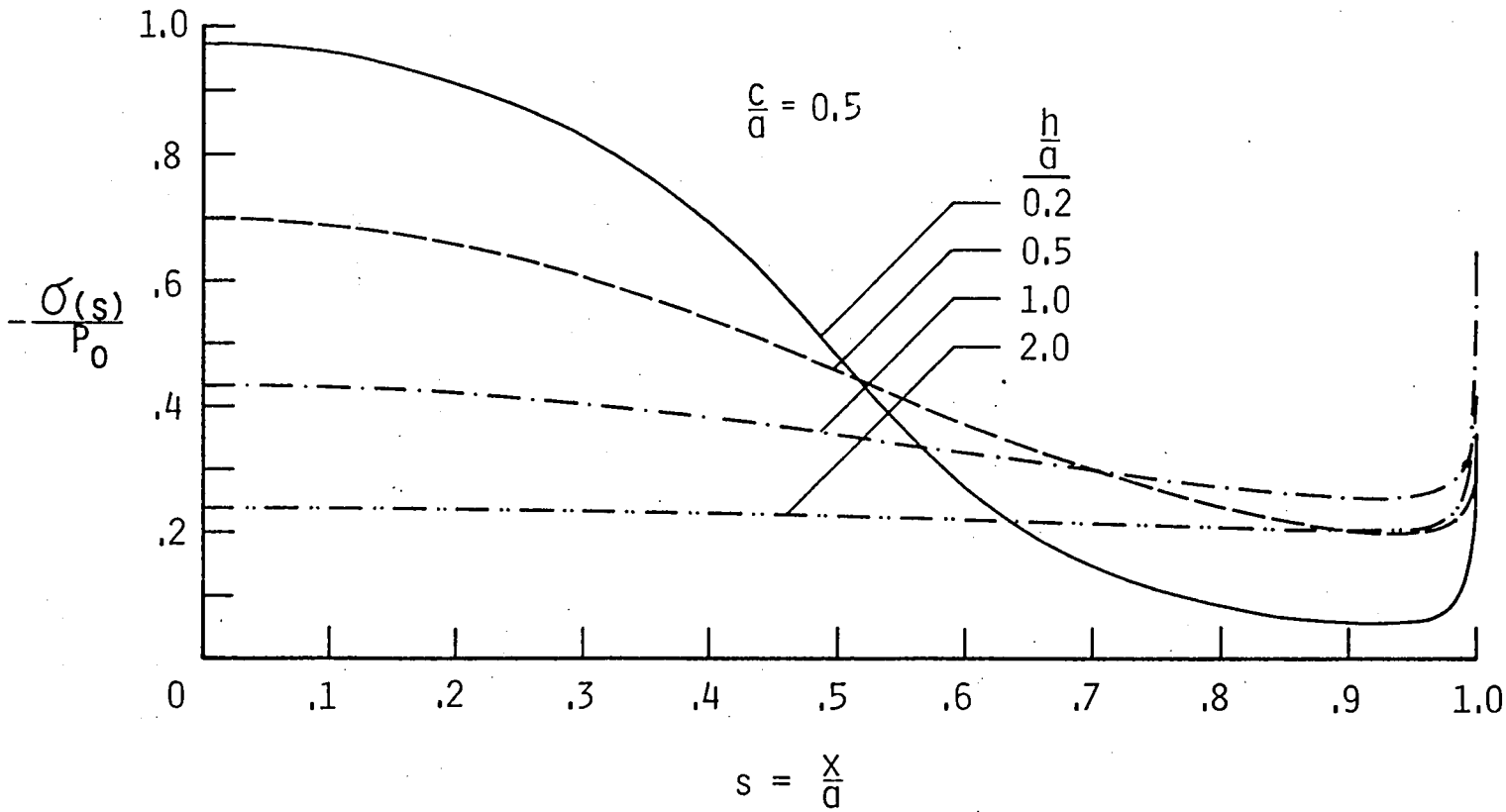

Figure 2. Contact stress distribution for full contact between a steel layer and aluminum half-plane.

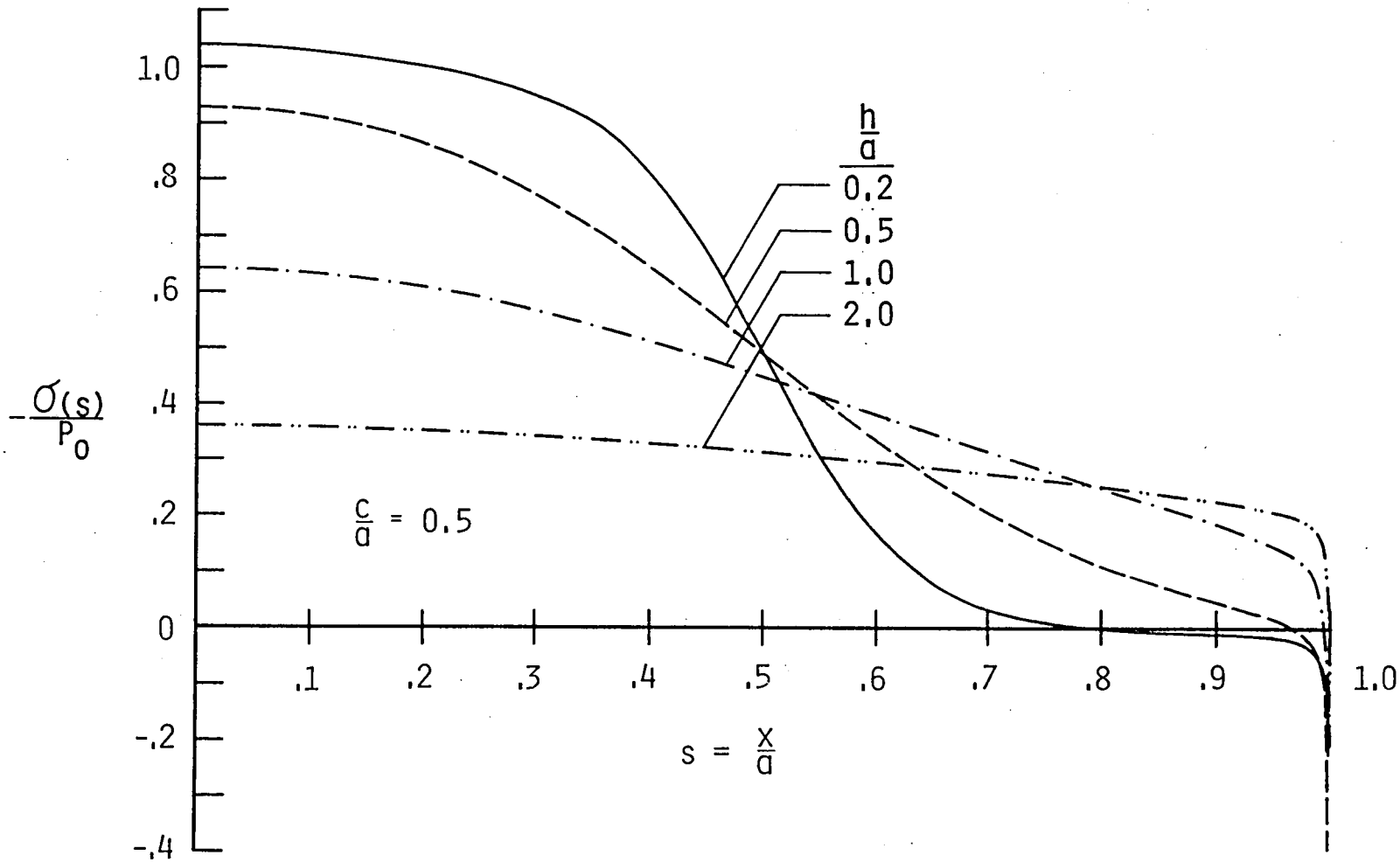

Figure 3. Contact stress distribution for full contact between an aluminum layer and steel half-plane.

Figure (4) shows the effect of the width c of the loaded region (relative to the crack length) on the contact stress; the contact stress is plotted versus position on the crack for several values of $\frac{c}{a}$. All the results are for an aluminum layer and a steel half-plane. The magnitude of the contact stress increases as the width of the loaded region increases, but the singular stress remains tensile, even for a $\frac{c}{a}$ value greater than one.

Figures (2), (3), and (4) establish several important trends in the behavior of the full-contact problem which can be carried forward to the discussion of the singular stresses at the crack-tips and later to the partial-contact problem: (1) the sign of the singular stress at the crack-tip depends on the relative stiffness of the layer and the half-plane; (2) changing the layer thickness to crack length ratio changes the contact stress distribution but not the sign of the singularity; and (3) changing the load width to crack length ratio changes the contact stress distribution but not the sign of the singularity.

Using Equation (95), stress intensity factors for the material combinations of Figures (2) and (3) are plotted in Figures (5) and (6) as a function of dimensionless load width. One should note that k_1 is not the classical mode I stress intensity factor but is the coefficient of the singular component of the contact stress on the unbonded side rather than the stress on the bonded side. The figure shows that for both material combinations and various values of $\frac{h}{a}$, the stress intensity factors increase to a maximum near $\frac{c}{a} = 1.0$ and then decay asymptotically to zero. Further, for both material combinations k_2 is much greater in magnitude than k_1.

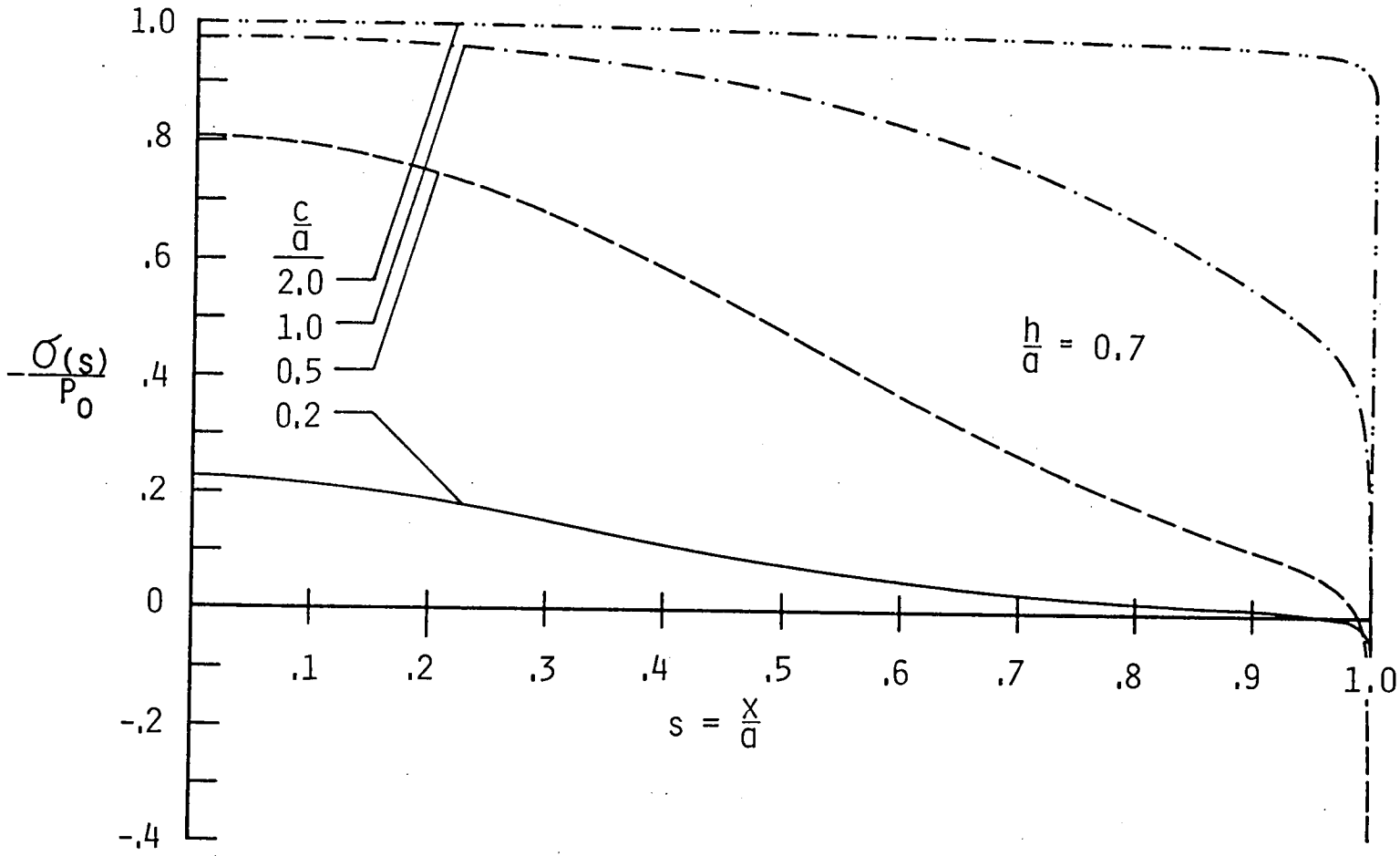

Figure 4. Variation of the contact stress distribution with $\frac{c}{a}$ for full contact between an aluminum layer and steel half-plane ($\frac{h}{a}$ = 0.7).

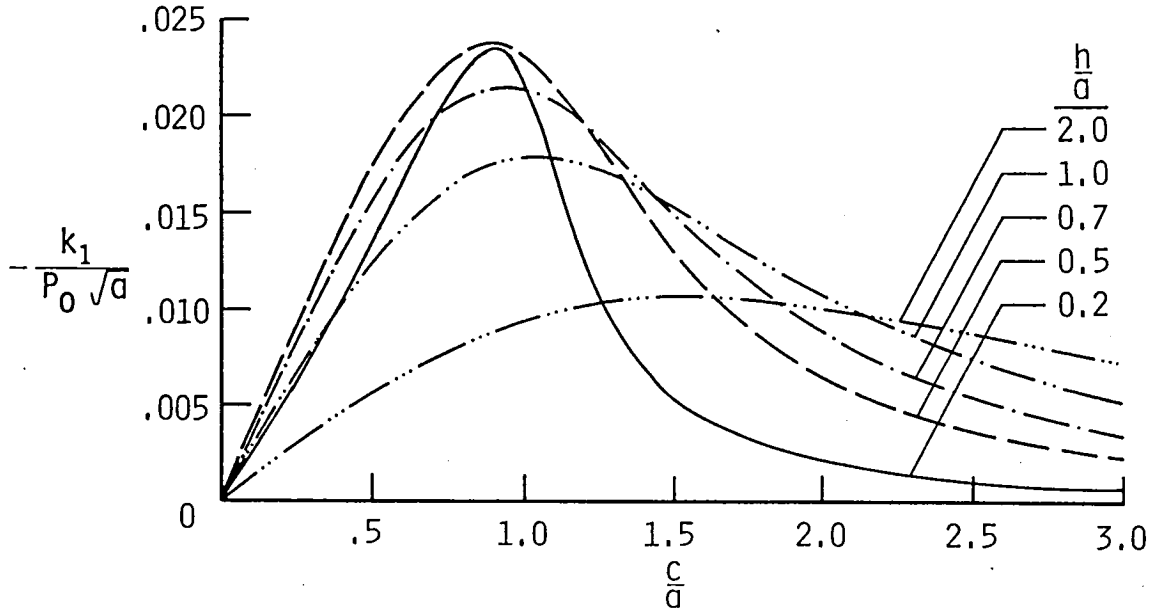

a. Coefficient of the singular contact stress.

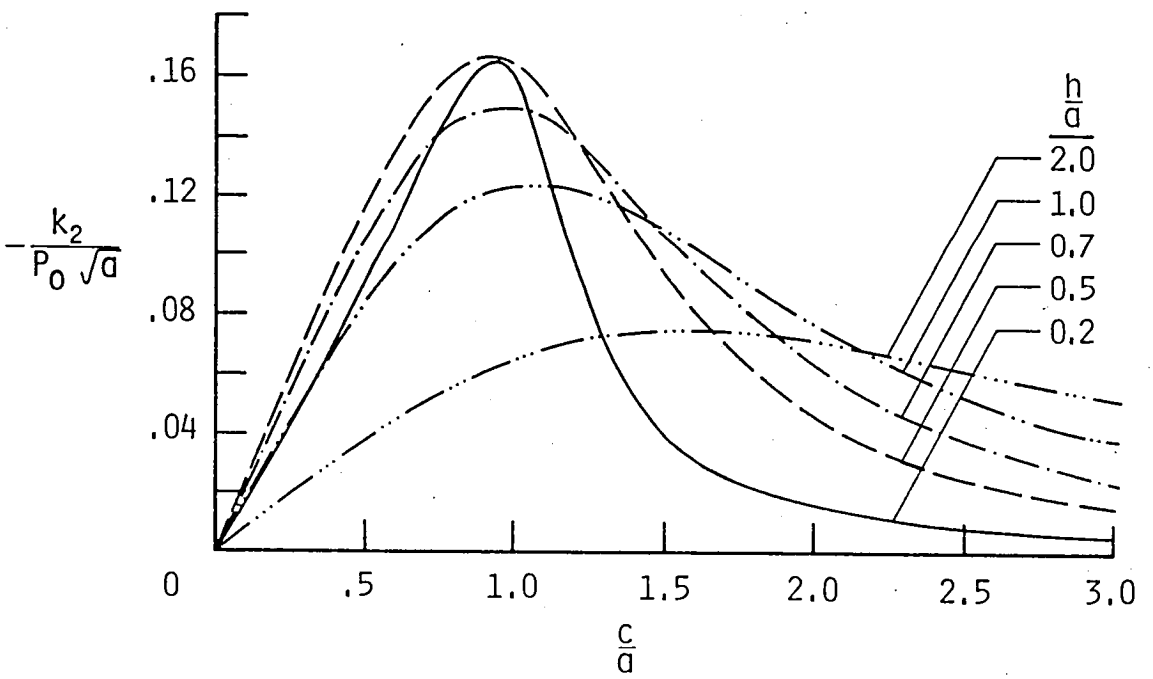

b. Mode II stress intensity factor.

Figure 5. Variation of the coefficients of the singular stress with $\frac{c}{a}$ for full contact of a steel layer and aluminum half-plane.

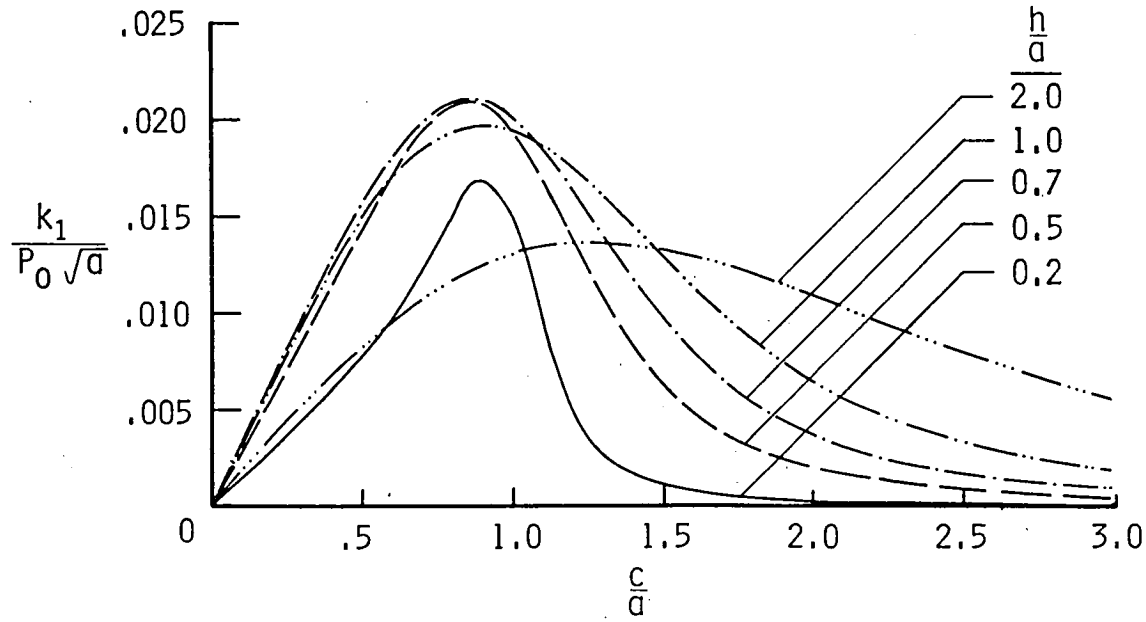

a. Coefficient of the singular contact stress.

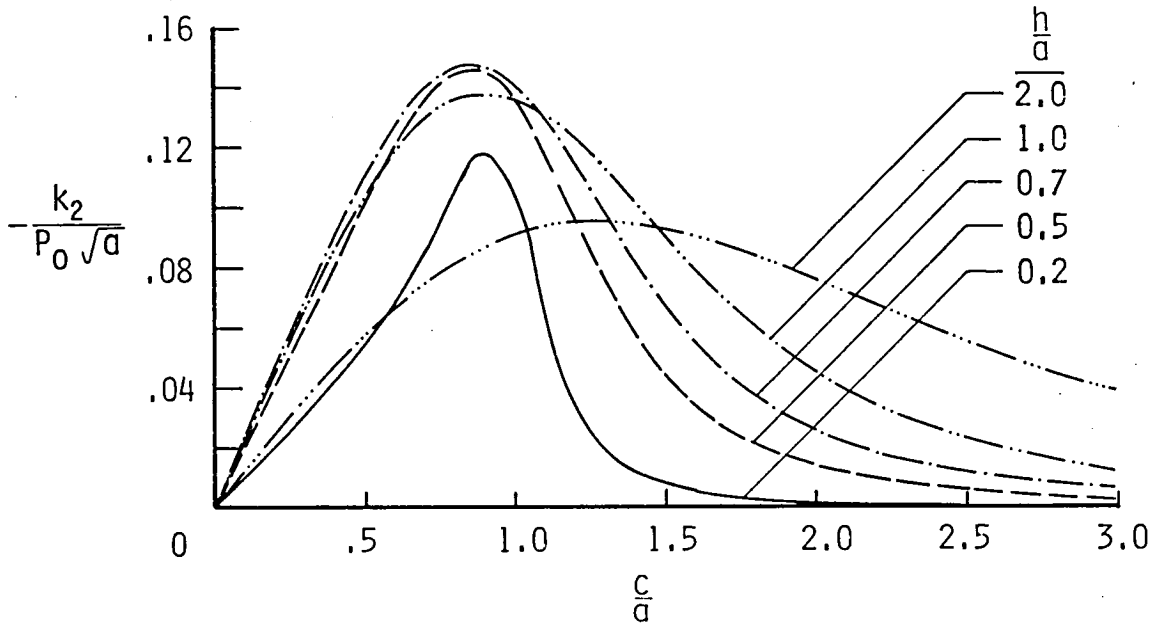

b. Mode II stress intensity factor.

Figure 6. Variation of the coefficients of the singular stress with $\frac{c}{a}$ for full contact of an aluminum layer and steel half-plane.

The sign of k_1 reflects the sign of the singular stress at the crack-tips. For the aluminum layer and steel half-plane the singular stress is tensile and k_1 is positive; for the steel layer and aluminum half-plane the stress is compressive and k_1 is negative. This indicates that for a relatively "soft" (aluminum) layer the no-separation constraint actually does prevent the layer from separating from the half-plane. For a relatively stiff layer the stresses at the crack-tips are compressive, but for small $\frac{h}{a}$ and $\frac{c}{a}$ there can be a region of tensile stress, which suggests the possibility of crack opening in the partial-contact problem. Interestingly, k_2 is negative for both material combinations, which indicates that the shear stress along the bond line constrains the layer from moving away from the origin relative to the half-plane, no matter which material is stiffer.

With k_1^{max} and k_2^{max} defined as the maximum k_1 and k_2 for a given $\frac{h}{a}$ (note that k_1^{max} and k_2^{max} are functions of $\frac{c}{a}$), Figure (7) shows k_1^{max} and k_2^{max} plotted versus $\frac{h}{a}$ for both material combinations. The peak values occur at $\frac{h}{a} \cong 0.4$ for the steel layer, aluminum half-plane combination and at $\frac{h}{a} \cong 0.7$ for the aluminum layer, steel half-plane combination. For large $\frac{h}{a}$, k_1^{max} and k_2^{max} become very small because of load diffusion effects.

Figure (8) shows k_1^{max} and k_2^{max} plotted against the stiffness ratio, E_1/E_2 for several values of $\frac{h}{a}$. For $E_1/E_2 > 1$, k_1^{max} is negative, and for $E_1/E_2 < 1$, k_1^{max} is positive (Figure (8a)). This indicates that at the crack-tip the layer is attempting to pull away from the half-plane only when $E_1/E_2 < 1$. The magnitude of k_1^{max} is largest when the stiffnesses are different, i.e., $E_1/E_2 \approx 7$ or $E_1/E_2 \approx 0.1$. The mode II stress intensity factor, k_2^{max}, is negative for all values of E_1/E_2.

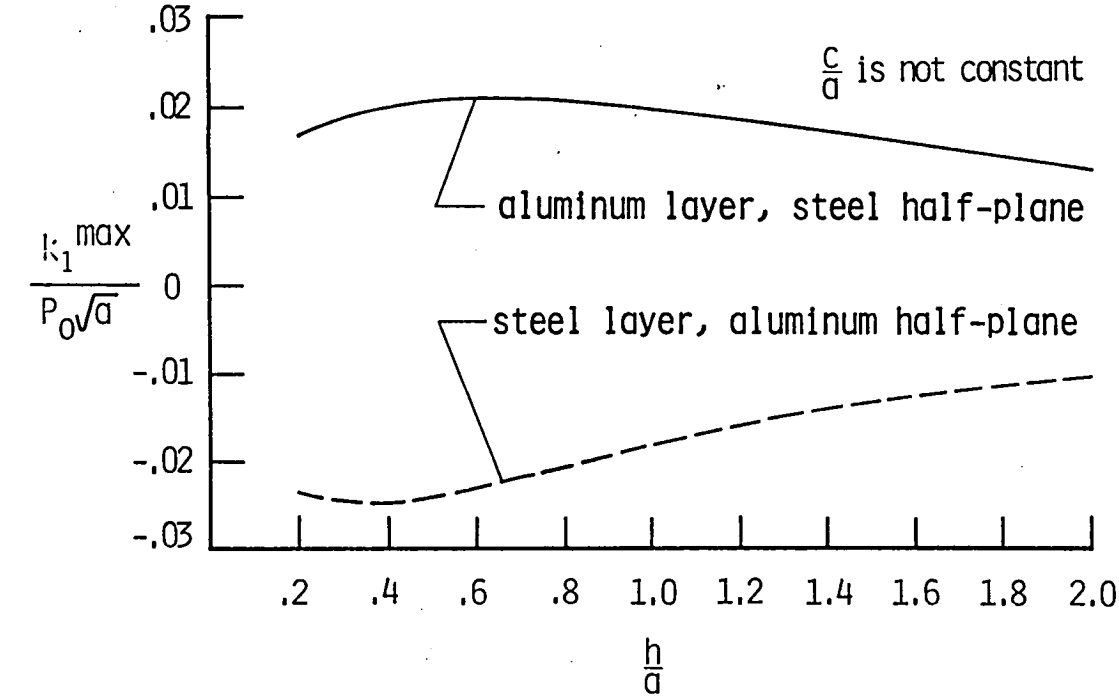

a. Coefficient of the singular contact stress.

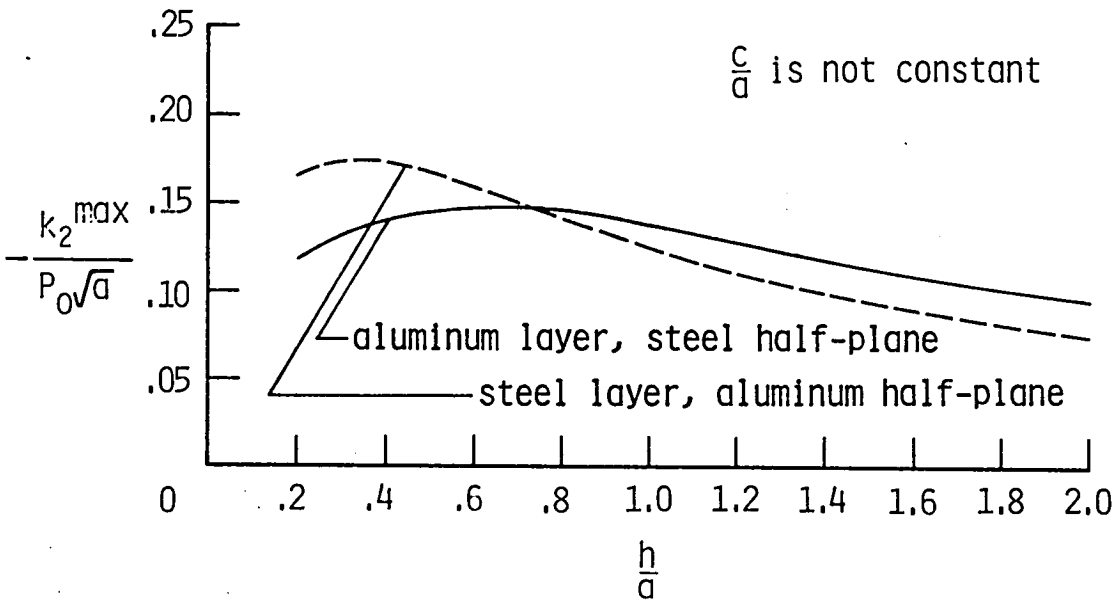

b. Mode II stress intensity factor.

Figure 7. Variation of the maximum coefficients of the singular stress with layer thickness, $\frac{h}{a}$, for the full-contact problem.

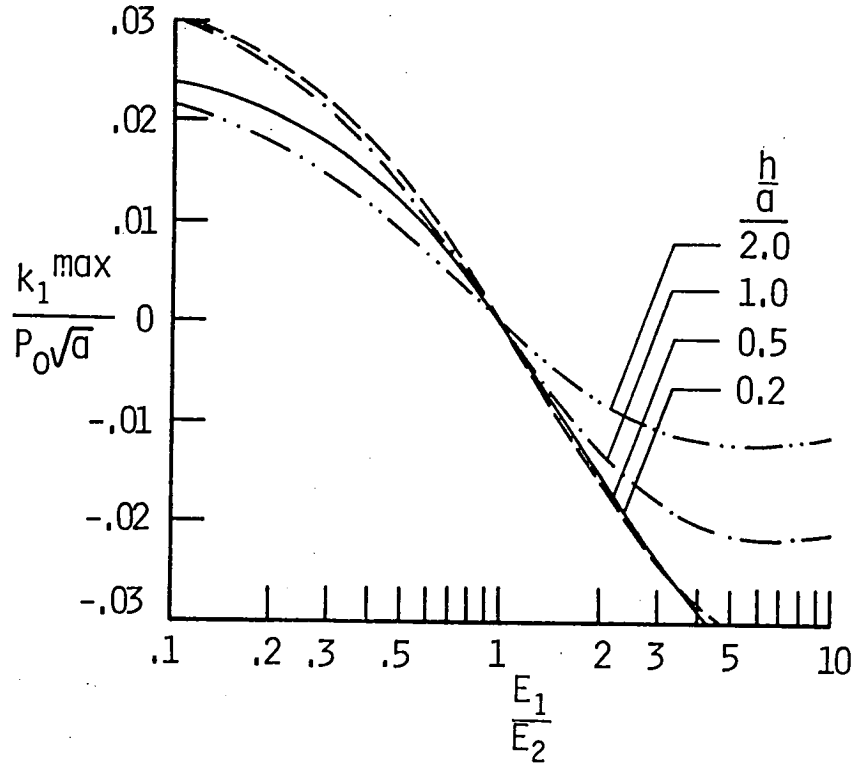

a. Coefficient of the singular contact stress.

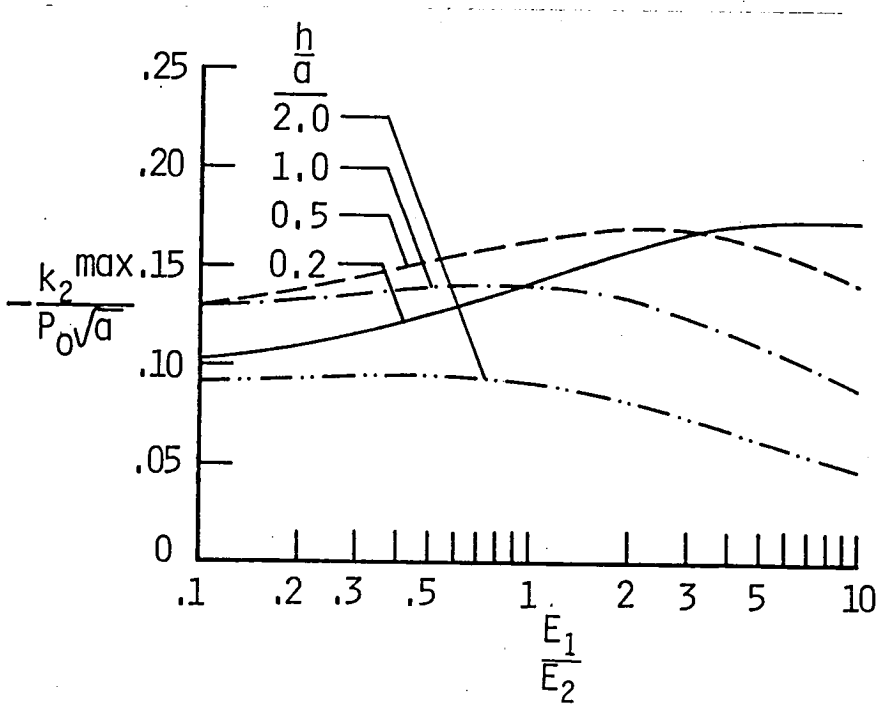

b. Mode II stress intensity factor.

Figure 8. Variation of the maximum coefficients of the singular stress with material stiffness ratio for the full-contact problem.

For $E_1/E_2 \to 0$, k_2^{max} appears to approach a single value for all values of $\frac{h}{a}$, but that has not been established here. For $E_1/E_2 \to \infty$, k_2^{max} tends toward zero because the layer is rigid relative to the half-space. For an ideally rigid layer k_1^{max} and k_2^{max} are zero because a finite load on an infinite rigid layer will produce zero displacement at the interface.

Partial Contact in the Region (-a,a)

In this problem the layer is allowed to separate from the half-plane at the ends of the crack (see Figure (1a)); the formulation and solution are in Chapters II and III. As discussed in Chapter II, the governing simultaneous equations are ill-conditioned and, consequently, solutions are obtained by satisfying the equations in the least-squares sense. The condition of the system of equations is found to depend on the combination of geometric parameters as well as the material properties of the layer and half-plane. As a result, satisfactory solutions are obtained for a relatively limited range of parameters, compared with the full-contact problem. To obtain solutions for a wider range of parameters would require more terms in the series expansion for ϕ (Equation (81)). However, the number of terms used to obtain the results presented herein required the maximum amount of storage available on the computer employed.

Figure (9) shows the contact stress and normal displacement difference distributions for an aluminum layer and steel half-plane. The contact stress vanishes at about $\frac{b}{a} = 0.61$. The normal displacement difference is essentially zero in the contact region, as required and the layer separates from the half-plane in the region of zero contact stress. The contact stress distribution is very similar to the compressive part of the distribution for the full-contact problem

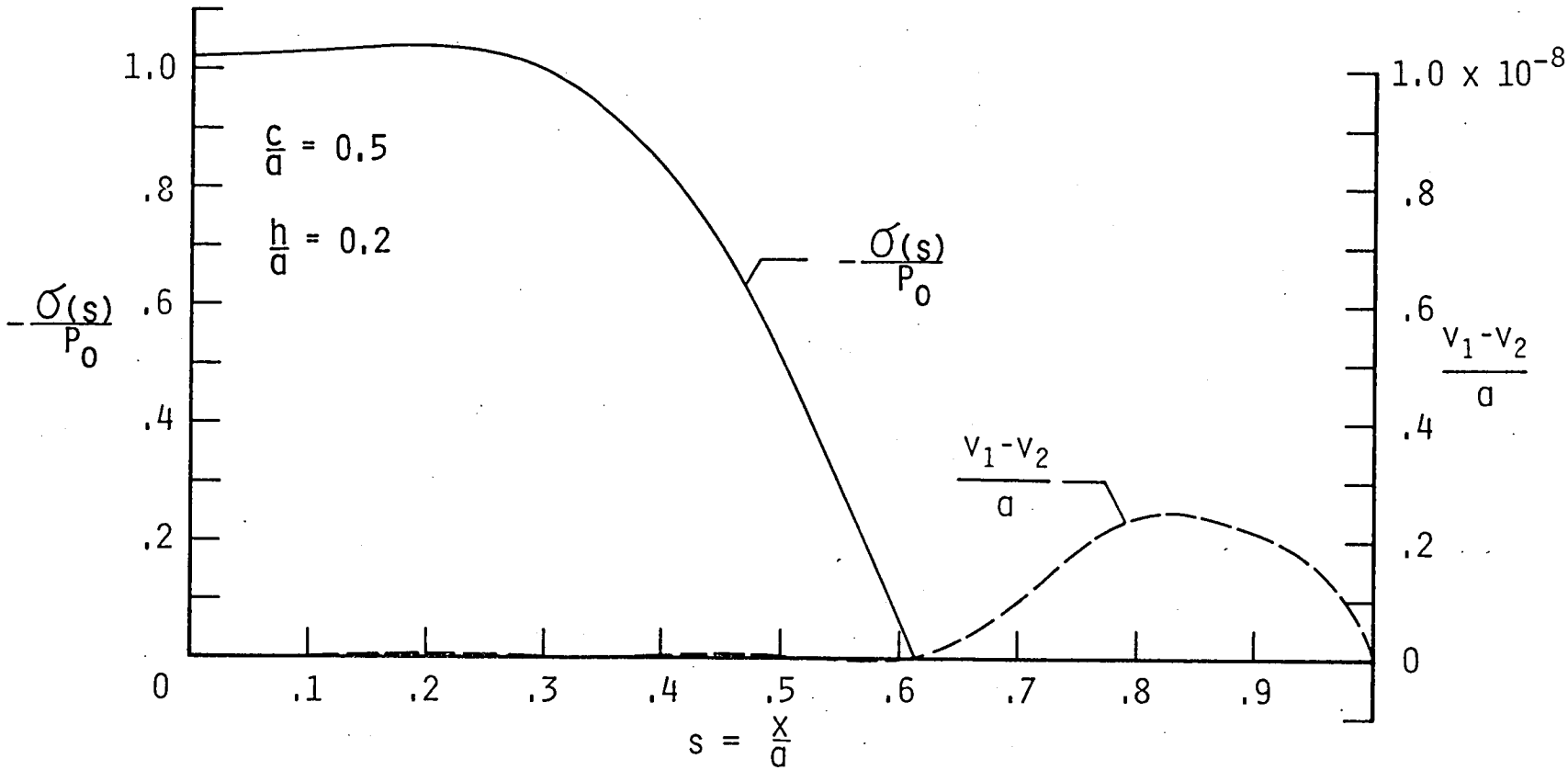

Figure 9. Contact stress and normal displacement difference distributions for partial contact between an aluminum layer and steel half-plane.

(see Figure (3)). In the full-contact problem, the stress changes sign at about $x = 0.79$, which is beyond the end of the contact zone in the partial-contact problem. The contact zone in the partial-contact problem should be smaller than the zone of compressive stress in the full-contact problem because, without the restraint imposed by the tensile stress of the full-contact problem, the crack will tend to open over an even greater area. Similar results were found for other combinations of geometric and material parameters.

The dimensionless half-width of the contact zone, $\frac{b}{a}$, as well as the magnitude of the contact stress and the crack opening, depend on the material and geometric parameters. Figure (10) shows the effect on $\frac{b}{a}$ of pressure distribution width, layer thickness, and material stiffness ratios. The size of the contact region increases with both layer thickness and pressure distribution width, but is insensitive to relative material stiffness for $E_1/E_2 < 1$. As the ends of the contact zone near the crack-tips, substantial error develops in the displacement differences on the interface. For example, a negative normal displacement difference is predicted at the ends of the contact zone for an almost closed crack. Because the crack faces cannot overlap, this is physically impossible. The error develops for large contact regions because the large region of zero displacement difference prevents the series expansion for ϕ from accurately modeling the small region of crack opening. For this reason, results are presented for relatively small $\frac{b}{a}$ and $\frac{c}{a}$.

The most important conclusion from the results for the partial-contact problem is that there is indeed crack opening near the ends of the crack under purely compressive external loading normal to the crack.

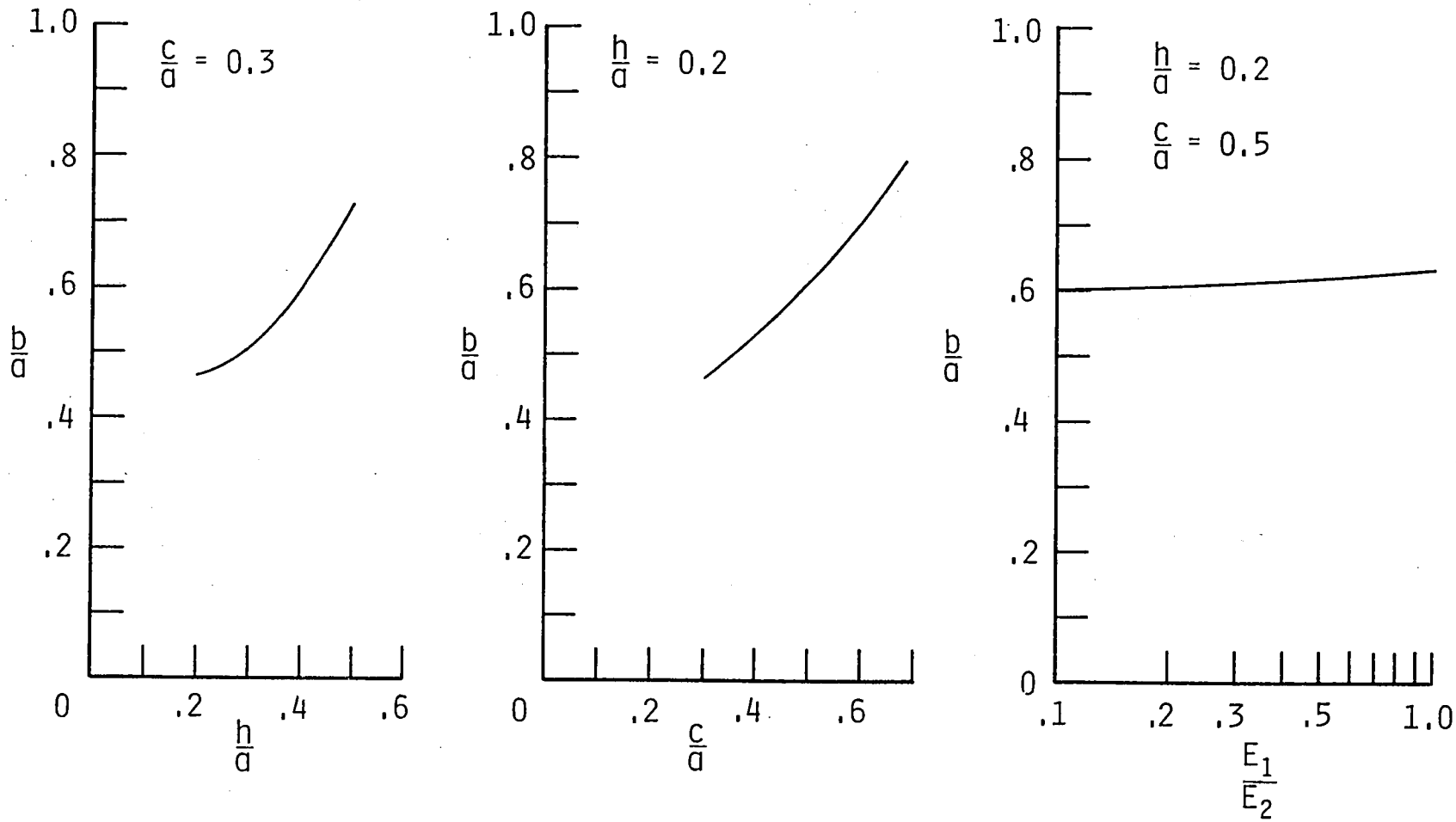

a. Effect of layer thickness.

b. Effect of pressure distribution zone width.

c. Effect of relative stiffness.

Figure 10. Variation of contact zone width with geometric and material parameters.

With crack opening comes the possibility of crack growth, and the likelihood of crack growth increases with the magnitude of the stress intensity factors. Figure (11) gives k_2 as a function of $\frac{h}{a}$ for several values of $\frac{c}{a}$, and as a function of E_1/E_2. Figure (11a) shows that k_2 increases with both layer thickness and the width of the region of applied pressure. These results are consistent with those of the full-contact problem over the same range of parameters. Figure (11b) shows that k_2 increases with the material stiffness ratio E_1/E_2. Again, these results are consistent with results from the full-contact problem. Results for k_1 are not presented because they appear to be of questionable accuracy. Computed values of k_1 are typically an order of magnitude smaller than the values of k_2, and thus are very sensitive to small errors in the series expansion of the displacement differences (which are used to compute k_1 and k_2). The apparent inaccuracy in k_1 does not change the important result that the crack does open which is consistent with a positive k_1. Because the normal displacement difference is closely related to k_1 and it is constrained in the contact zone, k_1 should be much smaller in magnitude than k_2. This is in fact the case, although the values of k_1 are suspect for the reasons mentioned above.

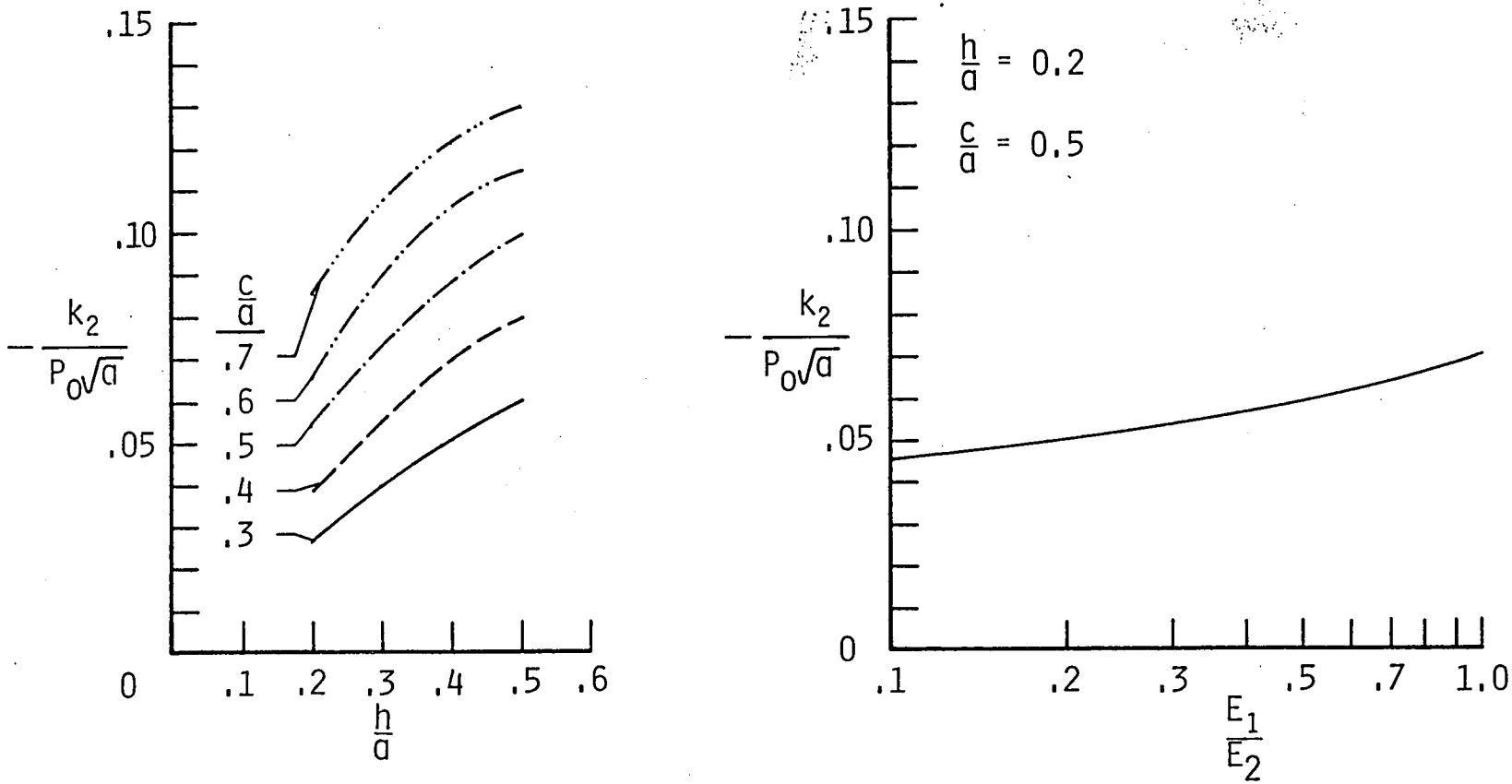

a. Effect of layer thickness and pressure distribution zone width.

b. Effect of relative stiffness.

Figure 11. Variation of partial-contact k_2 with geometric and material parameters.

CHAPTER V

CONCLUSIONS

The problem of an elastic layer bonded, except for a frictionless crack, to a dissimilar elastic half-plane is considered in this study to investigate the behavior of the disbond under compressive loading. Using Fourier transforms, the two-dimensional elasticity equations are converted to a pair of coupled singular integral equations with Cauchy-type kernels. The equations are reduced to a set of simultaneous algebraic equations which are ill-conditioned; as a result, the equations are solved in the least-squares sense. From the analysis, the following general conclusions about interface cracks in layered media are reached.

1. Under a normal pressure distribution on the free surface of the layer the tips of the crack can open. The resulting stresses at the crack-tips are singular, implying that crack growth is possible even under compressive loading.

2. The width of the crack-face contact zone depends on the layer thickness, the pressure distribution width, and the relative material properties of the layer and half-plane.

3. Crack-tip stress intensity factors depend on the geometric and material parameters.

4. Because the final set of simultaneous algebraic equations is ill-conditioned, accurate answers cannot be obtained for some values of the geometric and material parameters. To obtain accurate answers for a wider range of parameters, the program would have to be modified to allow for even more terms in the series expansion of the displacement-difference function.

APPENDICES

Appendix A

Material Property Terms

The expressions for the material property terms in Equations (28), (29), and (30) are

$$a_{11} = -(\mu_1 \kappa_2 + \mu_2)(\mu_1 + \mu_2 \kappa_1) ,$$

$$a_{12} = 4(\mu_1 \kappa_2 + \mu_2)(\mu_1 - \mu_2) ,$$

$$a_{13} = 0 ,$$

$$a_{14} = 2\mu_1^2 \kappa_2 + \mu_1 \mu_2 (\kappa_1 - 1)(\kappa_2 - 1) - \mu_2^2 (\kappa_1^2 + 1) ,$$

$$a_{15} = (\mu_2 \kappa_1 - \mu_1 \kappa_2)(\mu_1 - \mu_2) ,$$

$$c_{11} = \frac{1}{2} (\mu_1 \kappa_2 + \mu_2)(\kappa_1 + 1) ,$$

$$c_{12} = - \frac{1}{4} \mu_2 (1 + \kappa_1)(\kappa_1 \kappa_2 - 1) ,$$

$$c_{13} = \frac{1}{2} (\mu_2 - \mu_1) \kappa_2 (\kappa_1 + 1) ,$$

$$c_{14} = \frac{1}{4} \mu_2 (\kappa_1 + 1)(\kappa_1 - \kappa_2) ,$$

$$c_{21} = - \frac{1}{2} \mu_1 \mu_2 (\kappa_1 \kappa_2 - 1) ,$$

$$c_{22} = -2\mu_1 \mu_2 (\kappa_2 + 1) ,$$

$$c_{23} = \mu_1 \mu_2 (\kappa_1 + 1)(\kappa_2 - 1) ,$$

$$c_{24} = \frac{1}{2} \mu_1 \mu_2 (\kappa_1 - 1)(\kappa_2 + 1) ,$$

$$c_{25} = \frac{1}{2} \mu_1 \mu_2 (\kappa_2 - \kappa_1) ,$$

$$c_{31} = \mu_1^2 \kappa_2 + \mu_1 \mu_2 \left[\kappa_1 \kappa_2 + \frac{1}{2} (1 - \kappa_1 \kappa_2) \right] ,$$

$$c_{32} = 4 \mu_1 \left[\frac{1}{2} \mu_2 (\kappa_2 - 1) - \mu_1 \kappa_2 \right] ,$$

$$c_{33} = \mu_1 \mu_2 (\kappa_1 + 1)(\kappa_2 + 1) ,$$

$$c_{34} = -2 \mu_1^2 \kappa_2 - \frac{1}{2} \mu_1 \mu_2 (\kappa_1 - 1)(\kappa_2 - 1) ,$$

$$c_{35} = \mu_1^2 \kappa_2 - \frac{1}{2} \mu_1 \mu_2 (\kappa_1 + \kappa_2) ,$$

$$d_{11} = 0 ,$$

$$d_{12} = - \frac{1}{2} (\mu_1 + \mu_2 \kappa_1)(\kappa_1 + 1) ,$$

$$d_{13} = (\mu_2 - \mu_1)(\kappa_1 + 1) ,$$

$$d_{14} = \frac{1}{2} (\mu_1 - \mu_2)(\kappa_1 + 1) ,$$

$$d_{21} - \mu_1 (\mu_1 + \mu_2 \kappa_1) ,$$

$$d_{22} = 4 \mu_1 (\mu_1 - \mu_2) ,$$

$$d_{23} = 2 \mu_1 \mu_2 (\kappa_1 + 1) ,$$

$$d_{24} = 2\mu_1\left[\mu_1 + \frac{1}{2}\,\mu_2(\kappa_1 - 1)\right] ,$$

$$d_{25} = \mu_1(\mu_2 - \mu_1) ,$$

$$d_{31} = \mu_1(\mu_1 + \mu_2\kappa_1) ,$$

$$d_{32} = 4\mu_1(\mu_2 - \mu_1) ,$$

$$d_{33} = 2\mu_1\mu_2(\kappa_1 + 1) ,$$

$$d_{34} = -2\mu_1^2 - \mu_1\mu_2(\kappa_1 - 1) , \quad \text{and}$$

$$d_{35} = \mu_1(\mu_1 - \mu_2) .$$

The definitions of the material property terms in the integral equations are

$$\beta_{11} = -c_{11} ,$$

$$\beta_{12} = \frac{1}{2}\,(1 + \kappa_2)\,d_{12} - c_{12} ,$$

$$\beta_{13} = \frac{1}{2}\,(1 + \kappa_2)\,d_{13} - c_{13} ,$$

$$\beta_{14} = \frac{1}{2}\,(1 + \kappa_2)\,d_{14} - c_{14} ,$$

$$\beta_{21} = \frac{1}{2}\,(1 + \kappa_2)\,d_{21} - c_{21} ,$$

$$\beta_{22} = \frac{1}{2}\,(1 + \kappa_2)\,d_{22} - c_{22} ,$$

$$\beta_{23} = \frac{1}{2}(1 + \kappa_2)\, d_{23} - c_{23} ,$$

$$\beta_{24} = \frac{1}{2}(1 + \kappa_2)\, d_{24} - c_{24} ,$$

$$\beta_{25} = \frac{1}{2}(1 + \kappa_2)\, d_{25} - c_{25} ,$$

$$\beta_{31} = \frac{1}{2}(1 + \kappa_2)\, d_{31} - c_{31} ,$$

$$\beta_{32} = \frac{1}{2}(1 + \kappa_2)\, d_{32} - c_{32} ,$$

$$\beta_{33} = 0 ,$$

$$\beta_{34} = \frac{1}{2}(1 + \kappa_2)\, d_{34} - c_{34} ,$$

$$\beta_{35} = \frac{1}{2}(1 + \kappa_2)\, d_{35} - c_{35} ,$$

$$\beta_{41} = c_{11} - \frac{1}{2}(\kappa_2 - 1)\, d_{11} ,$$

$$\beta_{42} = c_{12} - \frac{1}{2}(\kappa_2 - 1)\, d_{12} ,$$

$$\beta_{43} = c_{13} - \frac{1}{2}(\kappa_2 - 1)\, d_{13} ,$$

$$\beta_{44} = c_{14} - \frac{1}{2}(\kappa_2 - 1)\, d_{14} ,$$

$$\beta_{51} = c_{21} - \frac{1}{2}(\kappa_2 - 1)\, d_{21} ,$$

$$\beta_{52} = c_{22} - \frac{1}{2}(\kappa_2 - 1)\, d_{22} ,$$

$$\beta_{53} = c_{23} - \frac{1}{2}(\kappa_2 - 1)\, d_{23} ,$$

$$\beta_{54} = c_{24} - \frac{1}{2}(\kappa_2 - 1)\, d_{24} ,$$

$$\beta_{55} = c_{25} - \frac{1}{2}(\kappa_2 - 1)\, d_{25} ,$$

$$\beta_{61} = c_{31} - \frac{1}{2}(\kappa_2 - 1)\, d_{31} ,$$

$$\beta_{62} = c_{32} - \frac{1}{2}(\kappa_2 - 1)\, d_{32} ,$$

$$\beta_{63} = c_{33} - \frac{1}{2}(\kappa_2 - 1)\, d_{33} ,$$

$$\beta_{64} = c_{34} - \frac{1}{2}(\kappa_2 - 1)\, d_{34} , \quad \text{and}$$

$$\beta_{65} = c_{35} - \frac{1}{2}(\kappa_2 - 1)\, d_{35} .$$

Appendix B

Relevant Integral and Limit Evaluations

The following integral formulas, all for $y < 0$, are taken from [14]:

$$\int_0^\infty e^{y\zeta} \sin(x\zeta)\sin(t\zeta)d\zeta = \frac{1}{2}\left[\frac{-y}{y^2 + (t-x)^2} - \frac{-y}{y^2 + (t+x)^2}\right],$$

$$\int_0^\infty e^{y\zeta} x\zeta \sin(x\zeta)\sin(t\zeta)d\zeta = -\frac{y}{2}\left[\frac{y^2 - (t-x)^2}{(y^2 + (t-x)^2)^2} - \frac{y^2 - (t+x)^2}{(y^2 + (t+x)^2)^2}\right],$$

$$\int_0^\infty e^{y\zeta} \sin(x\zeta)\cos(t\zeta)d\zeta = \frac{1}{2}\left[\frac{t+x}{y^2 + (t+x)^2} - \frac{t-x}{y^2 + (t-x)^2}\right],$$

$$\int_0^\infty e^{y\zeta} x\zeta \sin(x\zeta)\cos(t\zeta)d\zeta = y^2\left[\frac{t+x}{(y^2 + (t+x)^2)^2} - \frac{t-x}{(y^2 + (t-x)^2)^2}\right],$$

$$\int_0^\infty e^{y\zeta} \cos(x\zeta)\cos(t\zeta)d\zeta = -\frac{1}{2}\left[\frac{y}{y^2 + (t-x)^2} + \frac{y}{y^2 + (t+x)^2}\right], \text{ and}$$

$$\int_0^\infty e^{y\zeta} x\zeta \cos(x\zeta)\cos(t\zeta)d\zeta = -\frac{y}{2}\left[\frac{y^2 - (t-x)^2}{(y^2 + (t-x)^2)^2} + \frac{y^2 - (t+x)^2}{(y^2 + (t+x)^2)^2}\right].$$

The following evaluations of limits of certain integrals are taken from [14]:

$$\lim_{x \to 0^-} \int_0^\infty \psi(t)\left[\frac{y}{y^2 + (t-x)^2} \pm \frac{y}{y^2 + (t+x)^2}\right] dt = -\pi\psi(y),$$

$$\lim_{x \to 0^-} \int_0^\infty \psi(t) \left[\frac{y^3 - y(t-x)^2}{[y^2 + (t-x)^2]^2} \pm \frac{y^3 - y(t+x)^2}{[y^2 + (t+x)^2]^2} \right] dt = 0 \ , \quad \text{and}$$

$$\lim_{x \to 0^-} \int_0^\infty \psi(t) \left[\frac{y^2(t+x)}{[y^2 + (t+x)^2]^2} - \frac{y^2(t-x)}{[y^2 + (t-x)^2]^2} \right] dt = 0 \ .$$

Appendix C

Solution of the Full Contact Problem

For the full contact problem described in Chapter II, Equations (59) and (60) reduce to

$$\frac{\pi\sigma_{yy_2}\big|_{y=0^-}}{2\mu_2} = \int_{-c}^{c} P_o(t) \int_0^\infty \kappa_{11}(\alpha)\cos(\alpha t)\cos(\alpha x)\,d\alpha\,dt + \pi\frac{\beta_{31}}{a_{11}} f_1(x) - \int_{-a}^{a} f_1(t) \int_0^\infty \kappa_{13}(\alpha)\cos(\alpha t)\cos(\alpha x)\,d\alpha\,dt , \tag{C.1}$$

and

$$\frac{\pi\sigma_{xy_2}\big|_{y=0^-}}{2\mu_2} = \int_{-c}^{c} P_o(t) \int_0^\infty \kappa_{21}(\alpha)\cos(\alpha t)\sin(\alpha x)\,d\alpha\,dt - \frac{\beta_{61}}{a_{11}}\int_{-a}^{a}\frac{f_1(t)}{t-x}\,dt - \int_{-a}^{a} f_1(t) \int_0^\infty \kappa_{23}(\alpha)\cos(\alpha t)\sin(\alpha x)\,d\alpha\,dt . \tag{C.2}$$

The only continuity condition is Equation (63),

$$\int_{-a}^{a} f_1(x)\,dx = 0 . \tag{C.3}$$

The only independent unknown in the problem is f_1; $\sigma_{yy_2}\big|_{y=0}$ is now a function of f_1. Thus, the solution for f_1 is obtained from Equations (C.2) and (C.3).

Restricting x to the interval (-a,a) and defining

$$r = \frac{t}{a}, \qquad s = \frac{x}{a}, \quad \text{and}$$

$$g_1(s) = -f_1(as) = -f_1(x) ,$$

Equations (C.2) and (C.3) become

$$-\frac{1}{\pi}\frac{a_{11}}{\beta_{61}}\int_{-c}^{c} P_o(t)\int_0^{\infty} \kappa_{21}(\alpha)\cos(\alpha t)\sin(as\alpha)d\alpha\, dt = \frac{1}{\pi}\int_{-1}^{1}\frac{g_1(r)}{r-s}dr$$

$$+\frac{a}{\pi}\frac{a_{11}}{\beta_{61}}\int_{-1}^{1} g_1(r)\int_0^{\infty}\kappa_{23}(\alpha)\cos(ar\alpha)\sin(as\alpha)d\alpha\, dr , \quad |s| < 1 , \tag{C.4}$$

and

$$\int_{-1}^{1} g_1(s)\, ds = 0 . \tag{C.5}$$

Equation (C.4) is a singular integral equation of the first kind (as defined in [12]), and the dominant part,

$$\frac{\beta_{61}}{a_{11}}\int_{-1}^{1}\frac{g_1(r)}{r-s}dr$$

determines the fundamental functional form of g_1 which is

$$g_1(s) = \frac{G_1(s)}{\sqrt{1-s^2}} \tag{C.6}$$

where G_1 is a bounded continuous function.

The numerical technique developed in [18] is used to solve Equations (C.4) and (C.5). Following [18] the bounded function G_1 is approximated as

$$G_1(s) \simeq \sum_{k=0}^{K} C_k\, T_k(s) \tag{C.7}$$

where T_k is the Chebyshev polynomial of the first kind. Then substituting Equation (C.6) into Equation (C.4) with use being made of Equation (C.5), the integral equation reduces to the set of simultaneous equations,

$$\frac{1}{N}\sum_{n=1}^{N} G_1(r_n)\left[\frac{1}{r_n - s_m} + k(s_m,r_n)\right] = R(s_m),\ m = 1,\ \ldots,\ N-1 \qquad (C.8)$$

where use has been made of the appropriate relations from [18] and where

$$k(r_m,s_n) = a\,\frac{a_{11}}{\beta_{61}}\int_0^\infty \kappa_{23}(\alpha)\cos(ar_n\alpha)\sin(as_m\alpha)\,d\alpha\ , \qquad (C.9)$$

$$R(s_m) = -\frac{1}{\pi}\frac{a_{11}}{\beta_{61}}\int_{-c}^{c} P_o(t)\int_0^\infty \kappa_{21}(\alpha)\cos(\alpha t)\sin(as_m\alpha)\,d\alpha\,dt\ , \qquad (C.10)$$

$$r_n = \cos\frac{\pi}{2N}(2n-1)\ , \quad \text{and} \qquad (C.11)$$

$$s_m = \cos\frac{\pi m}{N}\ . \qquad (C.12)$$

Equation (C.8) gives N - 1 equations for N unknowns; using the Gauss-Chebyshev integration formula [17], Equation (C.3) gives the N^{th} equation as

$$\frac{\pi}{N}\sum_{n=1}^{N} G_1(r_n) = 0\ . \qquad (C.13)$$

After determining $G_1(r_n)$ by solving Equation (C.8) and C.13), the stresses on the entire interface are computed using Equations (C.1) and (C.2). The stress intensity factors are computed from Equation (95) with $\alpha = -1/2$.

LIST OF SYMBOLS

a	half crack length
a_{ij}, c_{ij}, d_{ij}	functions of material properties as defined in Appendix A
b	half width of the contact zone
c	half width of the applied pressure region
E_1, E_2	Young's moduli of layer and half-plane, respectively
f_1, f_2	displacement-difference functions on u and v, respectively
g_1, g_2	dimensionless displacement-difference functions for f_1 and f_2, respectively
G_1	bounded continuous function defined in Equation (C.6)
h	layer thickness
i	$\sqrt{-1}$
k_1, k_2	coefficients of the singular stresses
$P_o(x)$	pressure distribution on the free surface of the layer
P_o	magnitude of the uniform applied pressure
$P_n^{(\alpha,\bar{\alpha})}$	nth order Jacobi polynomial
T_k, U_k	kth Chebyshev polynomial of the first and second kind, respectively
v_i, u_i	displacements in the ith material in the y and x directions, respectively
$w(x)$	weight function of the Jacobi polynomials
$\alpha, \bar{\alpha}$	superscripts in the Jacobi polynomials
β_{ij}	material property terms defined in Appendix A
Γ	gamma function
δ_1, δ_2	material property coefficients as defined by Equations (74) and (75)
κ_i	material property constant for the ith material

λ_i, μ_i Lame constants for the ith material

$\sigma(s)$ normal stress in the contact region

$\sigma_{xx_i}, \sigma_{yy_i}, \sigma_{xy_i}$ stresses in the ith material

$\sigma_{yy_{2|y=0^-}}$ normal stress in the y-direction in the half-plane at y = 0

$\sigma_{xy_{2|y=0^-}}$ shear stress in the half-plane at y = 0

ϕ complex function of g_1 and g_2 defined by Equation (69)

ω material property term defined by Equation (80)

∇^2 Laplace differential operator

Subscripts

x,y Cartesian coordinates

1,2 layer and half-plane, respectively

REFERENCES

1. Rhodes, M. D. "Impact Tests on Fibrous Composite Sandwich Structures." NASA TM-78719. 1978.

2. Gladwell, G. M. L. Contact Problems in the Classical Theory of Elasticity. (Sijthoff & Noordhoff, Germantown, Maryland, 1980).

3. Ratwani, M. and F. Erdogan. "On the Plane Contact Problem for a Frictionless Elastic Layer." Int. J. Solids Structures. 9: 921-936. 1973.

4. Gecit, M. R. and F. Erdogan. "Frictionless Contact Problem for an Elastic Layer Under Axisymmetric Loading." Int. J. Solids Structures. 14: 771-785. 1978.

5. Civelek, M. B., F. Erdogan, and A. O. Cakiroglu. "Interface Separation for an Elastic Layer Loaded by a Rigid Stamp." Int. J. Engineering Science. 16: 669-679. 1978.

6. Civelek, M. B. and F. Erdogan. "The Axisymmetric Double Contact Problem for a Frictionless Elastic Layer." Int. J. Solids Structures. 10: 639-659. 1974.

7. Keer, L. M., J. Dundurs, and K. C. Tsai. "Problems Involving a Receding Contact Between a Layer and a Half Space." J. Applied Mechanics. 39: 1115-1120. 1972.

8. Keer, L. M. and K. Chantaramungkorn. "Loss of Contact Between an Elastic Layer and Half-Space." J. Elasticity. 2: 191-197. 1972.

9. Erdogan, F. and G. Gupta. "The Stress Analysis of Multi-Layered Composites With a Flaw." Int. J. Solids Structures. 7: 39-61. 1971.

10. Erdogan, F. and G. D. Gupta. "Layered Composites With an Interface Flaw." Int. J. Solids Structures. 7: 1089-1107. 1971.

11. Comninou, M. "The Interface Crack." J. Applied Mechanics. 44: 631-636. 1977.

12. Methods of Analysis and Solutions of Crack Problems. G. C. Sih, ed., (Leyden, Noordhoff International Pub., 1973).

13. MACSYMA Reference Manual. Version Nine, (Massachusetts Institute of Technology, Boston, Dec. 1977).

14. Erdogan, F. "Simultaneous Dual Integral Equations With Trigonometric and Bessel Kernels." Z. angew. Mathematik Mechanik, Band 48, Heft 4, 217-225. 1968.

15. Gradshteyn, I. S. and I. M. Ryzhik. Table of Integrals, Series, and Products. Corrected and enlarged edition, (Academic Press, Inc., NY, 1981).

16. Forsythe, G. E., M. A. Malcolm, and C. B. Moler. Computer Methods for Mathematical Computations. (Prentice-Hall, Inc., Englewood Cliffs, NJ, 1977).

17. Abramowitz, M. and I. A. Stegun. Handbook of Mathematical Functions With Formulas, Graphs, and Mathematical Tables. AMS 55, (U. S. Government Printing Office, Washington, D.C., 1964).

18. Erdogan, F. and G. D. Gupta. "On the Numerical Solution of Singular Integral Equations." Quarterly Applied Mathematics. 29: 525-534. 1972.

1. Report No.	2. Government Accession No.	3. Recipient's Catalog No.
NASA TM-86282		

4. Title and Subtitle	5. Report Date
Opening of an Interface Flaw in a Layered Elastic Half-Plane Under Compressive Loading	August 1984
	6. Performing Organization Code: 506-53-23-05
7. Author(s): John M. Kennedy, W. B. Fichter, and *James G. Goree	8. Performing Organization Report No.
9. Performing Organization Name and Address: NASA Langley Research Center, Hampton, VA 23665	10. Work Unit No.
	11. Contract or Grant No.
12. Sponsoring Agency Name and Address: National Aeronautics and Space Administration, Washington, DC 20546	13. Type of Report and Period Covered: Technical Memorandum
	14. Sponsoring Agency Code

15. Supplementary Notes

*James G. Goree, Clemson University, Clemson, SC

16. Abstract

This dissertation presents a static analysis of the problem of an elastic layer perfectly bonded, except for a frictionless interface crack, to a dissemilar elastic half-plane. The free surface of the layer is loaded by a finite pressure distribution directly over the crack. The problem is formulated using the two dimensional linear elasticity equations. Using Fourier transforms, the governing equations are converted to a pair of coupled singular integral equations. The integral equations are reduced to a set of simultaneous algebraic equations by expanding the unknown functions in a series of Jacobi polynomials and then evaluating the singular Cauchy-type integrals. The resulting equations are found to be ill-conditioned and, consequently, are solved in the least-squares sense.

Results from the analysis show that, under a normal pressure distribution on the free surface of the layer and depending on the combination of geometric and material parameters, the ends of the crack can open. The resulting stresses at the crack-tips are singular, implying that crack growth is possible. The extent of the opening and the crack-tip stress intensity factors depend on the width of the pressure distribution zone, the layer thickness, and the relative material properties of the layer and half-plane.

17. Key Words (Suggested by Author(s))	18. Distribution Statement
integral equations, elasticity, layered media, interface crack, singular stresses	Unclassified - Unlimited Subject Category 39

19. Security Classif. (of this report)	20. Security Classif. (of this page)	21. No. of Pages	22. Price
Unclassified	Unclassified	72	A04

For sale by the National Technical Information Service, Springfield, Virginia 22161